June 2021

Prepared by Fasmatech & Karolinska Institute

CONTENTS

1. D2.3 – In situ testing of optimized ExD MS/MS

A schematic representation of the different experiments performed with intact mAbs and involving variable energy electrons is presented in **Figure 1**. The versatility of the ion-activation network available in the Omnitrap platform allows for selective injection of electrons with precisely controlled kinetic energy at any step of a multiple-stage tandem MS workflow. **Figure 2** shows the mass spectrum of denatured non-reduced trastuzumab with the charge state distribution extending from z≈40+ to z≈60+. For denatured analysis, buffer exchanged trastuzumab (Herceptin) was diluted to 5μM in water:acetonitrile in 50:50 ratio (v/v) with 0.1% formic acid. Static nanoelectrospray experiments were performed using pulled borosilicate glass coated emitters (Thermo Fisher Scientific) biased at 1.3 to 1.5KV. Typically, a stable signal was produced for 1-2 hrs by loading 2-3 μL onto the offline emitter. Mass selection at MS2 level was performed using the quadrupole mass filter of the Q-Exactive Plus Orbitrap mass spectrometer (Thermo Fisher Scientific) upgraded with the BioPharma option. Isolation at MS3 level was performed in the Omnitrap.

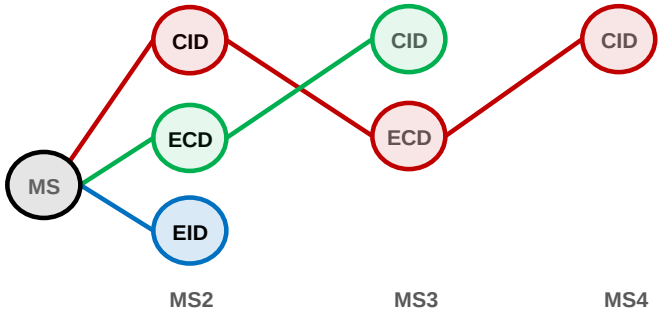

Figure 1. Ion activation network explored involving variable energy electrons for top down analysis of intact monoclonal antibodies.

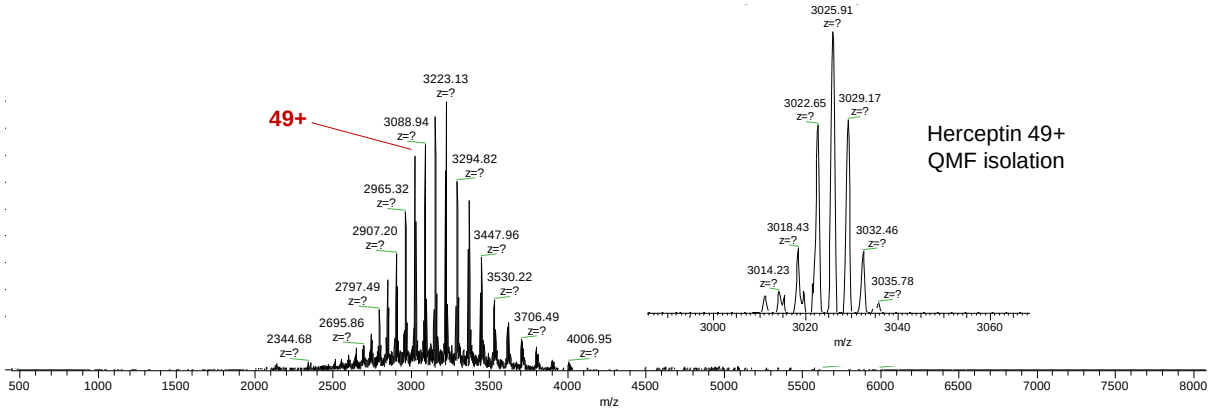

Figure 2. Mass spectrum of denatured trastuzumab (Herceptin) with 5μM concentration produced by static electrospray ionization. Charge state 49+ is selected using the quadrupole mass filter and injected in the Omnitrap platform for top down analysis.

1.1 MS2 Electron Capture Dissociation

Low energy electrons are produced by a heated tantalum disk-filament (Kimball Physics) operated at ~6.0A and injected through a 1.6 mm diameter aperture on the side pole-electrode of segment Q5. Multiply charged mAb ions are confined axially by applying a DC offset (2V) on neighboring segments and electron irradiation time is typically set to 150 ms. The electron current available for ECD in these experiments is of the order of 0.5 – 1.0 μA. **Figure 3** shows the averaged ECD

mass spectrum of the 49+ charge state precursor ions of trastuzumab. Extensive charge reduction is observed following capture of low energy electrons simultaneously with the formation of fragment ions extending across a wide mass range (500-2500 Th). ECD is performed at different q_z values (0.07, 0.1, 0.2 and 0.3 in the stability diagram) by adjusting the frequency of the rectangular RF waveform set at $250V_{0p}$ to extend the trapping range and enhance signal-to-noise of fragment ions on both ends of the mass spectrum.

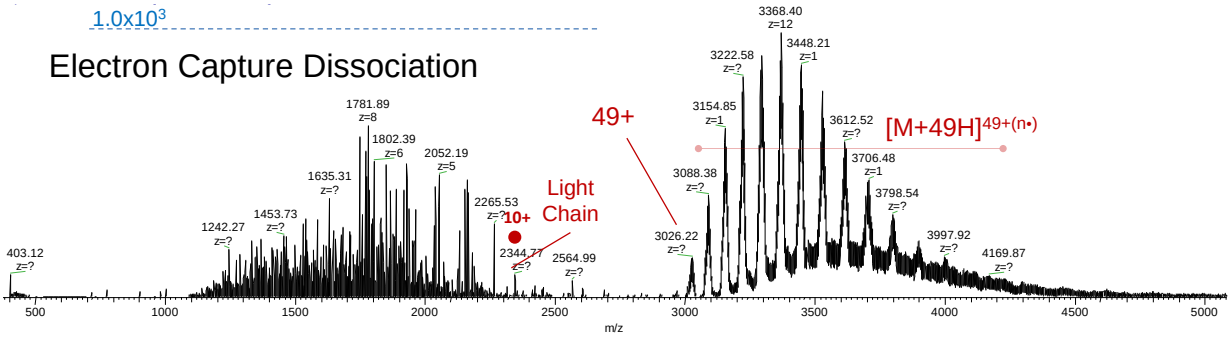

Figure 3. ECD mass spectrum of charge state 49+ producing charge-reduced precursor species and fragment ions. The mass spectrum is recorded using 5 µscans and a total of ~100 scans.

Data processing is performed in PeakFinder (Fasmatech) using the MS-Product (Protein Prospector) online fragment calculator modified for the TopSpec project to include multiply charged internal b- and a-type ions. Theoretical isotopic distributions are calculated based on the chemical formulas provided by the fragment calculator using the enviPat web 2.4 algorithm (Swiss Federal Institute of Aquatic Science and Technology) embedded in PeakFinder and fitted on the experimental data. Mass calibration is first performed in mMass. External calibration is performed using light chain fragments produced during ECD and also high abundance c ions that could be assigned with high confidence. **Figure 4** and **Table 1** show the results of the external mass calibration across the mass range where fragments are isotopically resolved and precise assignments can be made. Manual processing is performed in PeakFinder with new algorithms developed for fitting entire isotopic distributions on experimental data sets based on multiple scoring functions to maximize the confidence in the assignments. All data sets generated within the TopSpec project using the Omnitrap technology and applied for top down analysis of mAbs are analyzed using the procedure outlined here.

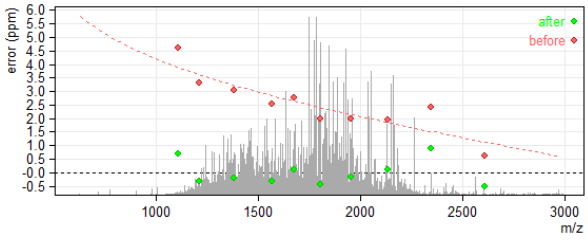

Figure 4. Mass calibration in mMass.

reference	theoretical	measured	calibrated	error before	error after
[M+10H]10+	2344.7600	2344.7657	2344.7621	2.4	0.9
[M+11H]11+	2131.7826	2131.7868	2131.7828	2.0	0.1
[M+12H]12+	1954.0510	1954.0550	1954.0507	2.0	-0.1
[M+13H]13+	1803.8938	1803.8974	1803.8931	2.0	-0.4
[M+14H]14+	1675.1162	1675.1209	1675.1164	2.8	0.1
[M+15H]15+	1563.5759	1563.5799	1563.5754	2.6	-0.3
[M+17H]17+	1379.7443	1379.7485	1379.7440	3.1	-0.2
[M+9H]9+	2605.2880	2605.2897	2605.2867	0.7	-0.5
c122 11+	1208.0632	1208.0672	1208.0628	3.3	-0.3
c122 12+	1107.4752	1107.4803	1107.4760	4.6	0.7

Table 1. List of ions used for external calibration.

ECD appears to cleave the intermolecular disulfide bond linking the heavy and light chains together. As a result, intact light-chain ions can be observed with charge states extending from

10+ to 17+. **Figure 5** shows the sequence coverage obtained in ECD of the denatured trastuzumab charge state 49+. Domains within linked cysteines are highlighted. Extensive fragmentation and sequence coverage is obtained in regions external to those linked by intramolecular disulfide bridges while no primary fragments have been identified that originate or terminate within the disulfide-linked domains. Primary fragments of the c, z and a type give a sequence coverage of 29.4% for the light chain, and 24.1% for the heavy chain. All assignments are made with ±6 ppm mass accuracy and the total signal intensity assigned to fragments is 66.4%. Additional data analysis of the ECD experiment performed in PeakFinder is provided in **Appendix I**.

Figure 5. Sequence coverage obtained in ECD of charge state 49+ trastuzumab ions.

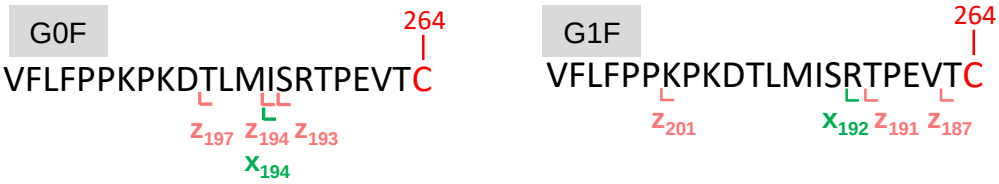

Figure 6. Aminoacid sequence between the 2nd and 3rd constant regions indicating the position of C-terminus fragments accommodating the glycan at Asn-300 in ECD of charge state 49+ ions.

A series of C-terminus heavy-chain fragments consisting of the second and third constant regions (C_{H2}, C_{H3}) of the Fc/2 domain of the antibody and also containing the glycan attached to Asn-300 have been identified. Sequence graphs indicating the position of these fragments including the G0F and G1F glycans are presented in **Figure 6**. Examples of mass spectra showing the theoretical isotopic distributions aligned with ECD G0F-containing fragments are presented in **Figure 7**. All the glycan-containing fragment ions identified in the ECD spectrum are low in intensity making the assignments rather difficult to make.

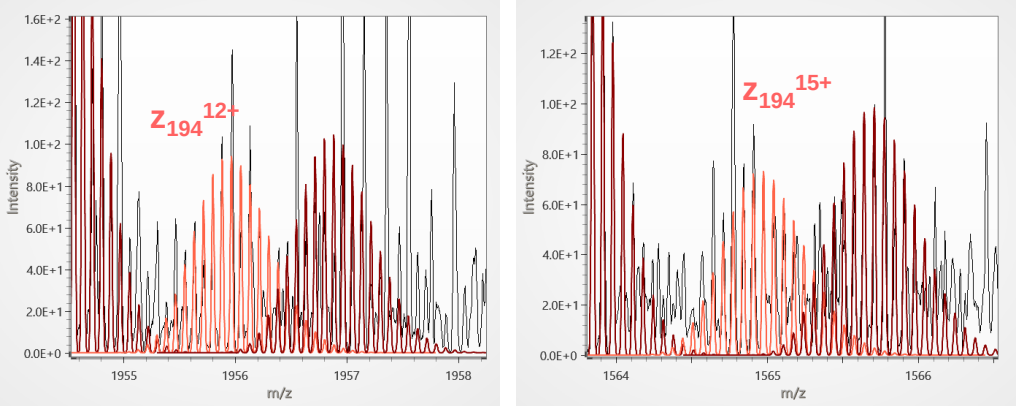

Figure 7. Examples of mass spectra showing the theoretical isotopic distributions of C-terminus heavy chain fragments containing the G0F glycan attached to Asn-300 superimposed on the ECD spectrum.

Extensive searches including all singly charged unidentified isotopic distributions to match either theoretical primary fragments accommodating the glycans, isolated glycan fragments or internal fragments accommodating the glycans have been performed without success in the MS2 CID spectrum. These searches must be extended in the ECD and collisionally-activated ECD data sets described here in an effort to identify fragmentation patterns that can be used in the analysis of other mAbs to enhance the characterization of these proteins by top down MS.

1.2 MS2 Collisionally Activated Electron Capture Dissociation

In addition to a plethora of lower m/z fragments, the MS2 ECD spectrum also comprises a series of charge-reduced precursor ions, which are not isotopically resolved and cannot be utilized to generate sequence information directly. A new workflow was developed in the Omnitrap platform where all ECD fragments generated in Q5 following irradiation by low energy electrons where transferred in segment Q2 and a broadband excitation signal was subsequently applied with excitation frequencies corresponding to the secular frequency of the high mass charge-reduced precursors. The application of the broadband excitation signal is synchronized with an argon gas pulse to promote collisional activation and dissociation of these species to generate additional lower m/z fragments and enhance sequence information. **Figure 8** shows the MS2 ECD spectrum presented above in **Figure 3** followed by collisional activation enabled by an 11 ms long broadband excitation signal designed with low frequencies and a step of 250 Hz. The MS2 ECD experiment is the average of multiple scans where different broadband excitation signals are applied and ranging from 10 KHz to 55 KHz to match the differences in ion secular frequencies

induced by variations in the RF drive frequency to extend the trapping mass range.

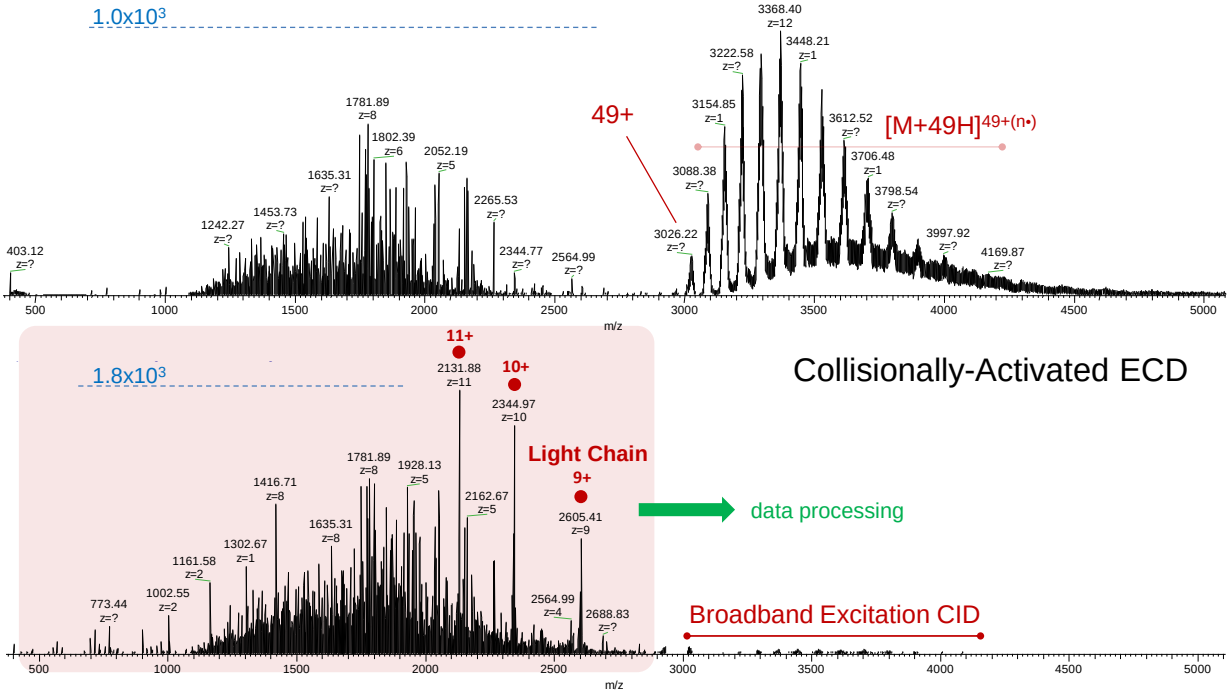

Figure 8. MS2 ECD of trastuzumab charge state 49+ in segment Q5 followed by collisional activation using broadband excitation during an argon gas pulse in segment Q2 to dissociate the isotopically unresolved charge-reduced high mass ECD precursor ions.

The most abundant fragments in the MS2 CA-ECD experiment are light chains ions with charge states extending from 8+ to 12+ indicating the high dissociation efficiency of the intermolecular SS bond. **Figure 9** shows light chains fragments formed in the MS2 CA-ECD experiment with charge states 11+, 10+ and 9+ where the intermolecular cysteine linkage is cleaved at three different positions, with the most abundant ion formed by dissociation of the disulfide bond.

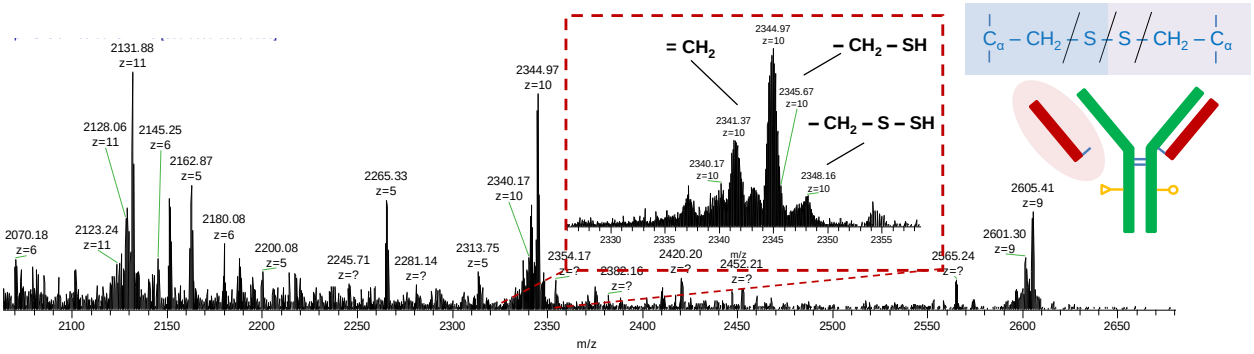

Figure 9. Light chain fragments formed in the MS2 CA-ECD of trastuzumab ions with charge state z=49+ highlighting the variations observed in the cleavage position of the intermolecular disulfide bond.

External mass calibration is performed in mMass using primary fragments and light chain ions listed in **Table 2** that can be assigned with high confidence across the entire m/z range of interest. **Figure 10** shows the mass accuracy obtained before and after external calibration.

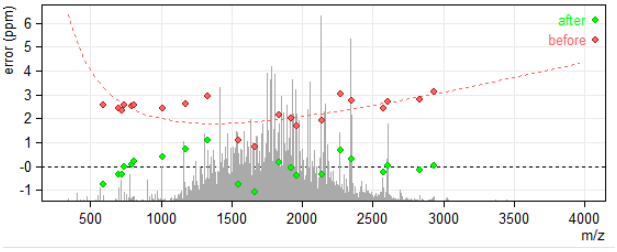

Figure 10. Mass calibration in mMass.

reference	theoretical	measured	calibrated	error before	error after
[M+10H]10+	2344.8600	2344.8665	2344.8608	2.8	0.3
[M+11H]11+	2131.6914	2131.6955	2131.6908	1.9	-0.3
[M+12H]12+	1954.2180	1954.2213	1954.2173	1.7	-0.4
[M+8H]8+	2930.6978	2930.7070	2930.6980	3.1	0.1
[M+9H]9+	2605.2880	2605.2952	2605.2881	2.8	0.1
b118 11+	1170.5915	1170.5946	1170.5924	2.6	0.8
b118 5+	2573.8921	2573.8984	2573.8915	2.4	-0.2
b5 1+	589.2650	589.2665	589.2646	2.6	-0.7
b6 1+ H	698.3719	698.3736	698.3717	2.4	-0.3
b7 + H	785.4040	785.4060	785.4041	2.5	0.1
b7 1+	804.3556	804.3577	804.3558	2.6	0.2
c101 6+	1833.2322	1833.2362	1833.2326	2.2	0.2
c104 4+	2831.3980	2831.4060	2831.3976	2.8	-0.1
c104 5+	2265.3190	2265.3260	2265.3206	3.1	0.7
c122 10+	1328.8687	1328.8726	1328.8702	2.9	1.1
c122 8+	1660.8344	1660.8358	1660.8327	0.9	-1.1
c123 7+	1916.2440	1916.2479	1916.2440	2.0	-0.0
c6 +	734.3502	734.3521	734.3502	2.6	-0.0
c6 + H	715.3985	715.4002	715.3983	2.4	-0.3
c9 +	1005.4670	1005.4695	1005.4674	2.4	0.4
c99 7+	1545.0458	1545.0475	1545.0447	1.1	-0.7

Table 2. List of ions used for external calibration.

Sequence coverage in the MS2 CA-ECD experiment is enhanced compared to the MS2 ECD experiment described in Section 1.1 above. New series of primary fragments external to the SS-linked domains are generated by broadband excitation of the charge-reduced ECD precursor ions, raising sequence coverage of the light chain to 41.6% and that of the heavy chain to 31.2%, as shown in **Figure 11**. Near-complete sequence coverage is obtained external to the SS protected domains of the light chain (96.6%), while the corresponding sequence coverage for the heavy chain is lower (68.7%) with the majority of unobserved cleavages located across the hinge region. Surprisingly, no assignments within the SS linked domain were possible except a few fragments located in the variable region of the light chain, indicating that intramolecular SS bonds cannot be reduced, neither in ECD nor in CA-ECD of the intact antibody. Dissociation of intramolecular SS bonds in CA-ECD is observed in an MS4 workflow involving the analysis of the light chain discussed in the following Section 1.3. Additional data analysis of the CA-ECD experiment is provided in **Appendix I**.

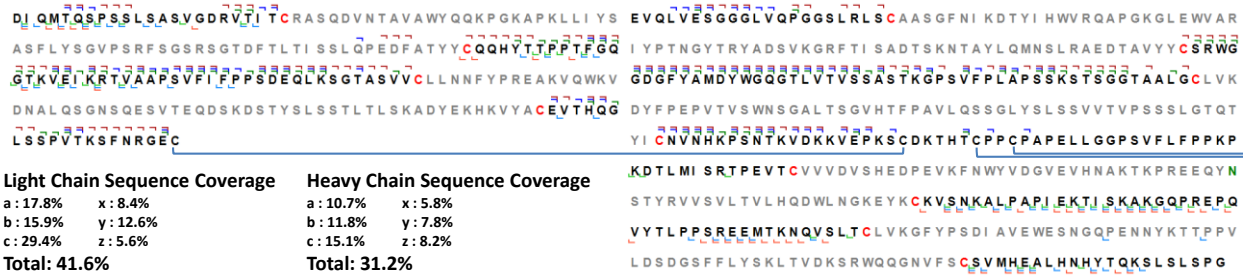

Figure 11. Sequence coverage obtained in CA-ECD of charge state 49+ trastuzumab ions.

C-terminus heavy-chain primary fragments (x, y and z) consisting of the second and third constant regions (C_{H2}, C_{H3}) of the Fc/2 domain of the antibody and also containing the glycan attached to Asn-300 have also been identified in MS2 CA-ECD. Sequence graphs indicating the position of these fragments, external to intramolecular SS bonded domains of the heavy chain including the G0F and G1F glycan modifications are presented in **Figure 12**. Examples of mass spectra

showing the theoretical isotopic distributions matched to G0F- and G1F-containing fragments are presented in **Figure 13**. Unfortunately, all isotopic distributions corresponding to fragments containing the glycan modification are located in highly congested regions of the MS2 CA-ECD mass spectrum and further isolation for MS3 analysis of these species is not feasible.

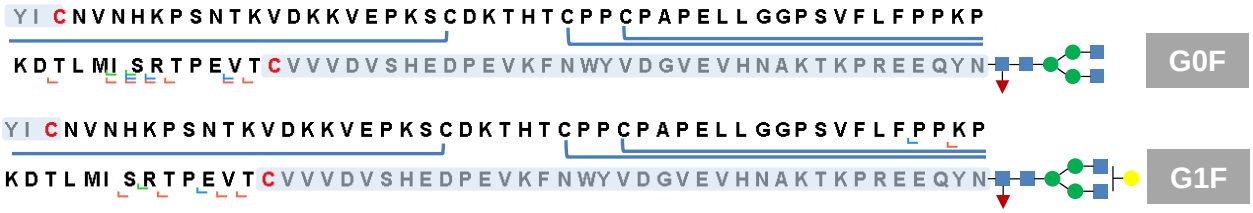

Figure 12. Sequence maps of the heavy chain near the hinge region of an IgG1-type mAb highlighting cleavage positions for C-terminus fragments containing the G0F and G1F modifications identified in the MS2 CA-ECD experiment.

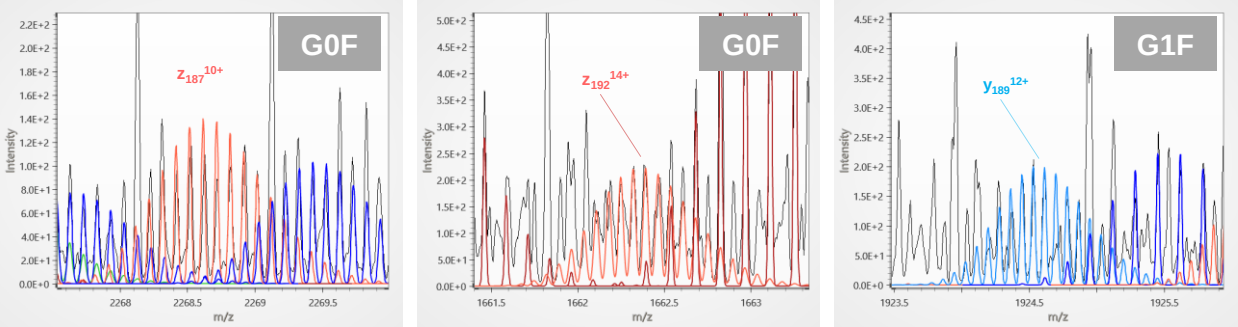

Figure 13. Examples of mass spectra showing the theoretical isotopic distributions superimposed on the CA-ECD spectrum of C-terminus heavy chain fragments containing the G0F and G1F glycan modifications attached to Asn-300.

1.3 MS4 Collisionally Activated Electron Capture Dissociation

The outstanding capabilities of the Omnitrap platform to support multiple-stage multi-dimensional tandem mass spectrometry workflows is demonstrated by an MS4 experiment involving ion accumulation. In contrast to MS2 experiments with peptides and small proteins where the number of fragmentation channels is rather limited, the precursor ion signal in top down analysis of large proteins is distributed over a significantly greater number of dissociation pathways resulting in low intensity fragments. These low signal-to-noise isotopic distributions observed in an MS2 experiment are difficult to assign while the problem is augmented further by the extreme spectral congestion typically encountered in top down of large protein systems. These two parameters, low signal-to-noise fragments and spectral congestion, preclude the development of multiple-stage tandem MS workflows that will permit in-depth characterization of intact proteins. By exploiting the unique performance characteristics of the Omnitrap platform, the problem is partly alleviated by isolating and accumulating selected fragment ions prior to performing the subsequent activation-dissociation step. Ion accumulation is performed at the expense of duty cycle, however, the level of information produced in such a workflow is remarkably rich.

Figure 14 shows the ion activation network available in the TopSpec Omnitrap platforms to be delivered at Karolinska and Pasteur. Also highlighted is the MS4 workflow developed specifically for the analysis of denatured non-reduced trastuzumab combining collisions with argon and low energy electrons. Alternative MS4 ion-activation pathways involving VUV photons have also been performed and results will be presented at the July 2021 Periodic Report. **Figure 15** shows a schematic representation of the MS4 processing cycle, indicating the position of the ions along the axis of the Omnitrap platform in each step of the sequence, and also highlighting the type of ion-activation or processing method applied. Mass spectra from each step of the processing cycle are presented and key features of this unique top down experimental workflow are discussed.

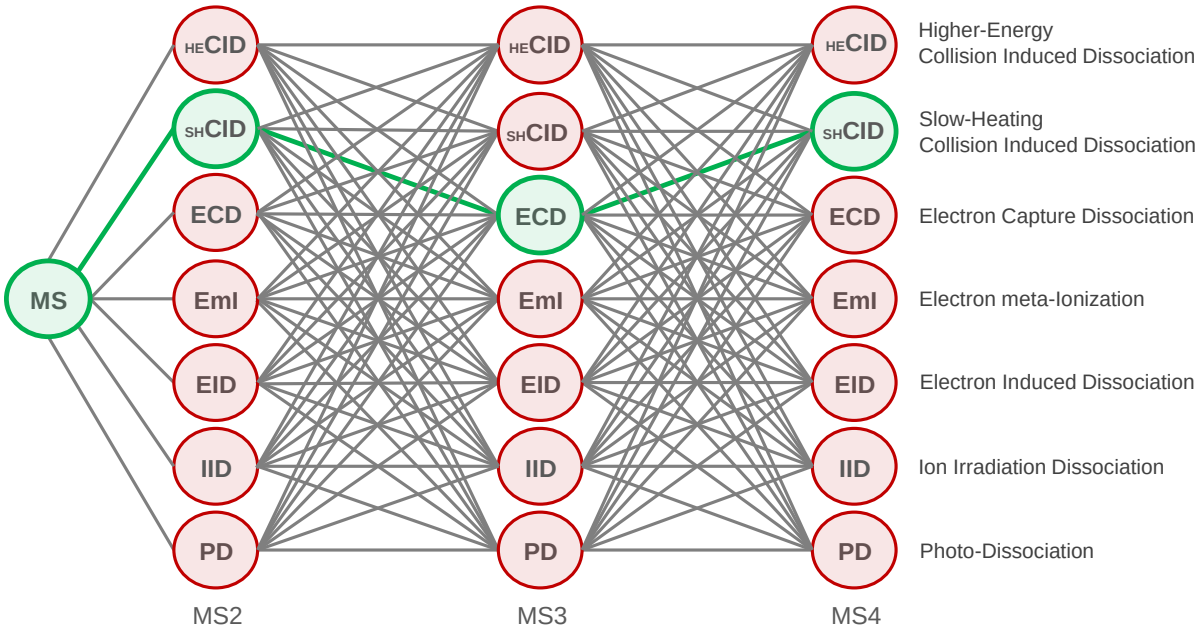

Figure 14. The ion activation network available in the TopSpec Omnitrap platforms includes collisions with buffer gas molecules, interactions with variable energy electrons, photons and fast ions. The MS4 workflow developed for top down analysis of intact monoclonal antibodies is highlighted.

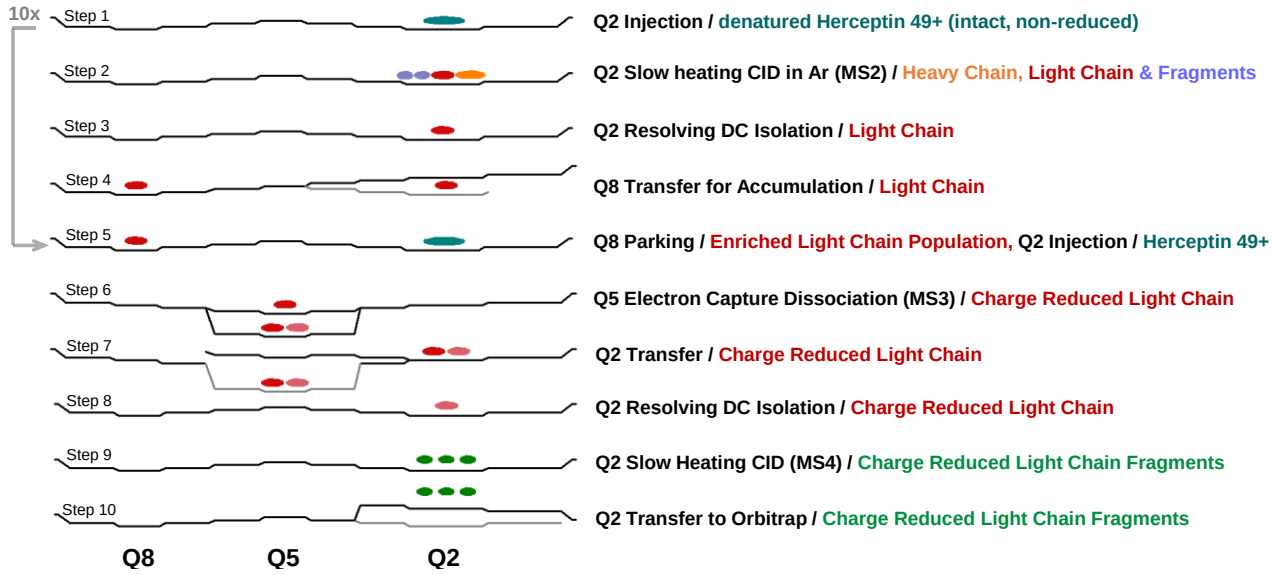

Figure 15. Sequence of ion processing events in the MS4 collisionally activated electron capture dissociation top down experiment for the analysis of intact mAbs.

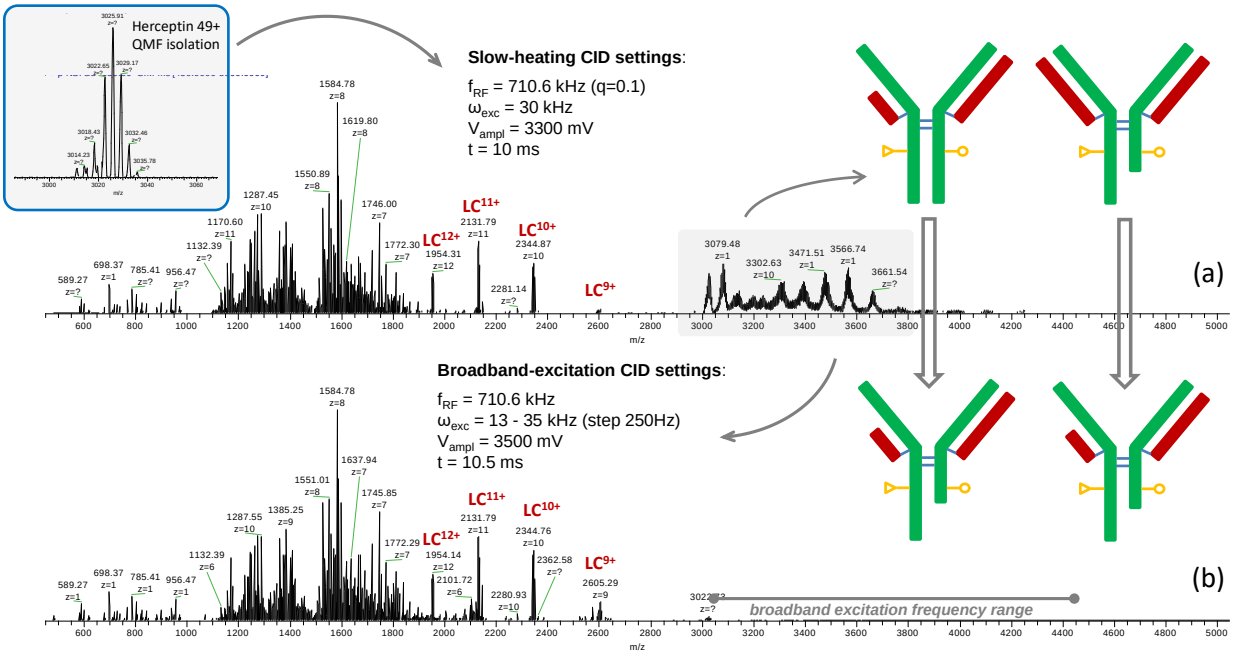

Figure 16. (a) Dipolar resonant excitation slow-heating CID of all glycosylated forms of intact trastuzumab 49+ ions followed by (b) dipolar broadband excitation of the high mass first-generation dissociation products that remain isotopically unresolved.

Figure 16 shows the MS2 two-step slow-heating CID spectra performed with the glycosylated trastuzumab ions corresponding to charge state z=49+. The first mass spectrum shown in **Figure 16 (a)** involves resonant excitation of all glycosylated forms of the 49+ ions producing a rich fragmentation pattern at m/z<2000 Th containing isotopically resolved species, intact light chain

dissociation products with charge states extending from 9+ to 13+ and also a series of non-resolved high mass dissociation products, complementary to the lower mass-to-charge ratio fragments. The second mass spectrum shown in **Figure 16 (b)** involves the application of a broadband excitation signal to dissociate further the isotopically non-resolved high mass fraction to enhance the signal to noise in the lower m/z region of the mass spectrum. Surprisingly, no new fragments are generated in the second CID step. In the first activation step an intact mAb will lose parts either from the light chain or the heavy chain, simultaneously producing two high mass complementary fragments as shown in **Figure 16 (a)**. Surprisingly, these high mass species exhibit the same dissociation pathways with those of the intact mAb, therefore, the second CID step will simply enhance the signal-to-noise of the first generation CID fragments without producing new information, as shown in **Figure 16 (b)**. Both resonant excitation and broadband excitation slow-heating CID steps are performed in an argon gas pulse raising pressure to >10^{-2} mbar for ~10 ms.

Slow-heating CID produces a considerably less congested spectrum compared to MS2 ExD experiments and allows for selecting fragment ions further for MSn interrogation with high efficiency. ECD, EID or UVPD appear less favorable as a starting step for developing MSn workflows since overlapping isotopic distributions generate isolation windows which contain undesired information. Dissociation of the intermolecular disulfide bonds has been reported in ECD and UVPD but not under typical slow-heating CID conditions, as observed here. Additional top down experiments with the NIST mAb have confirmed that SS bond dissociation by slow-heating CID for the IgG1 structure is more of a standard feature rather than a coincidence. Dissociation of the intermolecular SS bond was also observed in HCD fragmentation and results will be presented in the July 2021 periodic report.

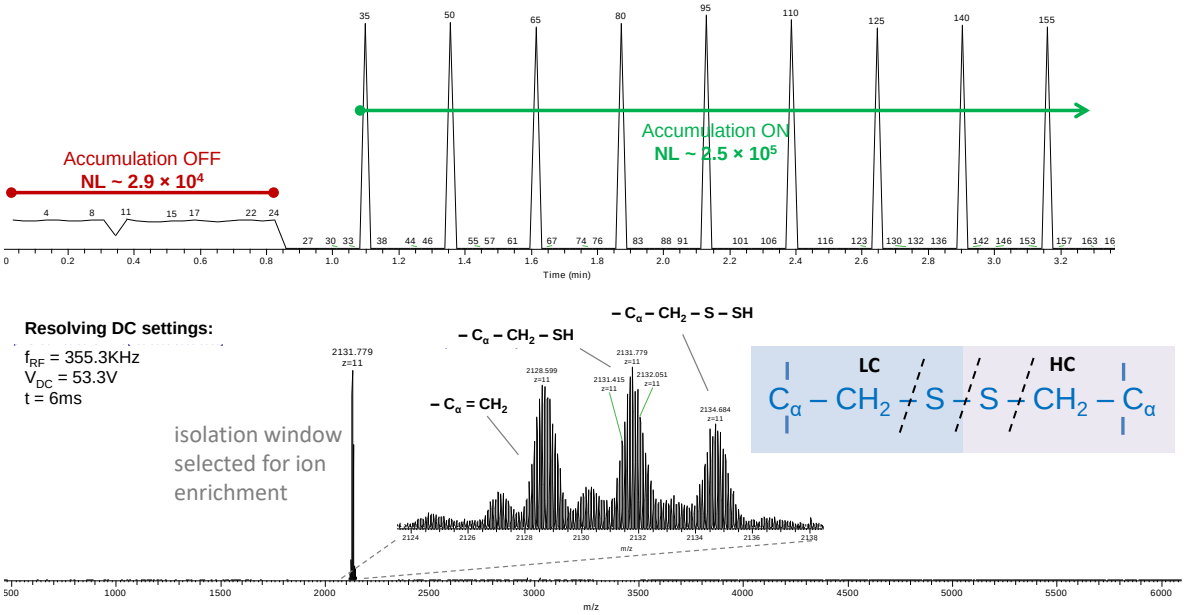

Figure 17. Accumulation of the light chain dissociation product ion is performed to enhance signal-to-noise and enable the MS4 workflow. The ion isolation window contains three main ions generated by differences in the cleavage position of the intermolecular SS bond.

The MS3 isolation window is presented in **Figure 17**. In this example, intact light chain ions with charge state z=11+ are selected by the application of a resolving DC signal applied to the pole-electrodes of segment Q2. The isolation window includes three main isotopic distributions identified as intact light chain ions with differences in the cleavage position across the intermolecular disulfide bond. The cleavage positions are located directly on the disulfide bond (S-S) between the two sulfur atoms, as well as between the β-carbons on the side chain of cysteines and sulfur (C_β-S) on either side of the intermolecular SS link. Secondary NH_3 losses are also observed for all three variations of the intact light chain dissociation products.

Figure 17 also shows the total ion current observed in Tune software (Thermo Fisher) during operation of the Omnitrap platform in normal and accumulation modes. Light chain ions produced and isolated in segment Q2 are transferred in segment Q8 for storage. The transfer-storage step is applied for a preselected number of consecutive scans performed by the Q Exactive instrument. During accumulation, the Orbitrap mass analyzer will return blank spectra since all ions are stored in Q8 instead of being transferred back to the HCD cell. Following a predetermined number of scans where no information is generated, the enriched population is transferred back to the HCD cell and a mass spectrum is produced with enhanced signal-to-noise ratio. Typically, an enhancement of the ion intensity by a factor of 10x is obtained for 15 accumulation scans. Experiments performed with 20 or more accumulation scans where not as successful.

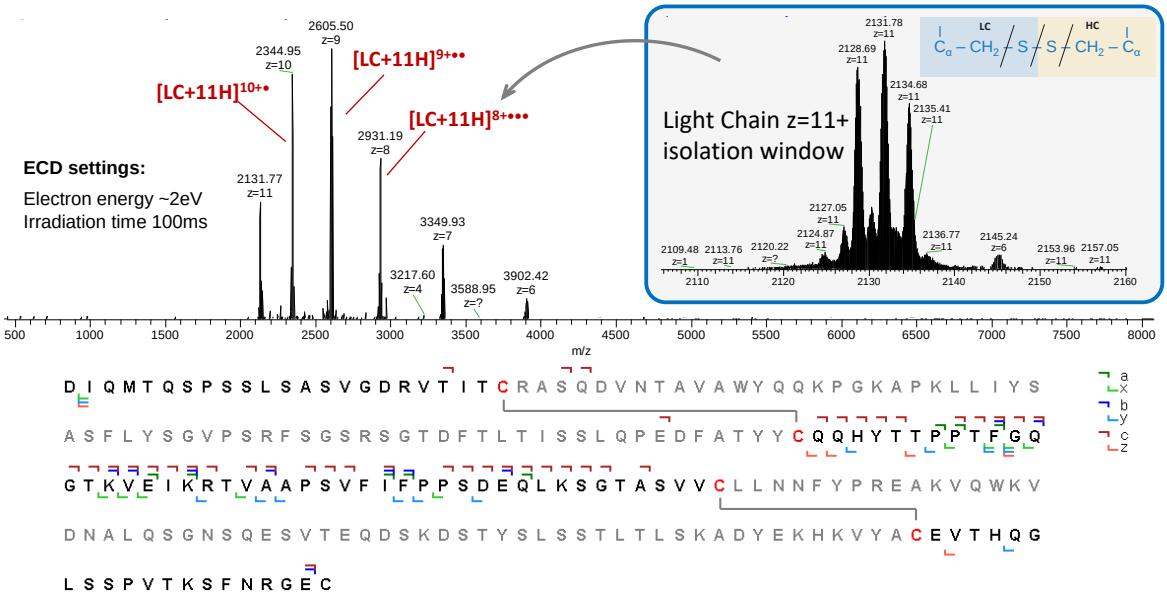

Figure 18. MS3 ECD mass spectrum showing charge-reduced light chain ions formed at short electron irradiation times and serving as the precursor species in the MS4 workflow. Also shown is the sequence coverage obtained by extending electron irradiation time to enhance dissociation of the light chain.

The accumulated population of light chain ions is subsequently transferred in segment Q5 and the potential energy of the ions relative to the filament potential is adjusted to enable interactions with slow energy electrons. Ions are transferred from segment Q8 during a gas pulse to thermalize ions kinetically at the center of Q5 and maximize the overlap with the electron beam. The arrival time of the ions is also synchronized with a gating potential applied to the steering optics of the

electron source to allow external injection of electrons into the RF trapping region at the desired time window. Charge-reduced ECD precursor ions are formed within 100 ms and the intensity of the elector beam is estimated at ~1 µA. **Figure 18** shows charge-reduced light chain ions formed with a maximum uptake of five electrons. Extending electron irradiation time to >100 ms reduces the intensity of the charge-reduced light chain ions while low abundance fragment ions are formed. In ECD experiments where electron irradiation time was prolonged to promote dissociation, a series of primary fragments were identified and located mainly between the two intramolecular disulfide bridges of the light chain, indicating that ECD alone is not sufficient to reduce the SS bond. For the MS4 experiments electron irradiation time was optimized to maximize the intensity of the charge-reduced light chain ions. **Figure 18** also shows the sequence coverage obtained by extending the period of ECD to >100 ms.

An example of the final MS4 isolation step followed by collisional activation of selected charge-reduced light chain ions $[M+11H]^{(11-n)+(n\bullet)}$ where n corresponds to the number of electrons captured by the ions is presented in **Figure 19** for charge state z=9+••. The isolation window includes mainly a triplet configuration of light chain radical ions produced by differences in the cleavage position across the intermolecular disulfide bond. The isolation window appears rather congested due to the presence of additional overlapping isotopic distributions attributed to side chains losses from the charge-reduced light chain ions, similarly to the ammonia losses observed in the MS2 CID experiment of the intact mAb described above. A narrower isolation window will become available and facilitate spectral assignments when the new rectangular RF generator operated at $400V_{0p}$ is installed. In the current experimental setup, the RF generator is limited to $250V_{0p}$. Also shown in **Figure 19** is the MS4 collisionally activated ECD spectrum of the $[M+11H]^{9+\bullet\bullet}$ ions where an abundance of fragments ions are generated across a wide mass range extending from 500 Th to 4000 Th. Additional MS4 CA ECD experiments were performed with the $[M+11H]^{10+\bullet}$ light chain ions. The sequence coverage, intensity and charge state distribution plots of fragment ions obtained for the two MS4 CA ECD experiments performed with the light chain are presented in **Appendix II**.

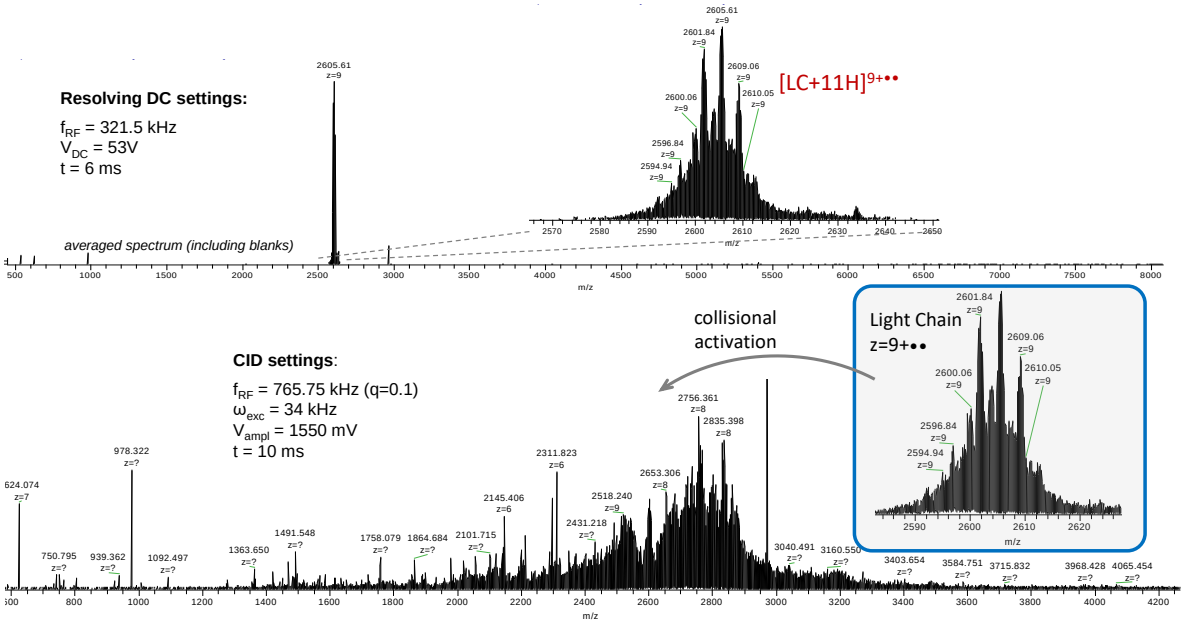

Figure 19. Mass spectra showing the isolated charge-reduced light chain ions formed by electron capture at MS3 level and the MS4 CA-ECD mass spectrum with fragment ions extending over an extended mass range.

The sequence coverage obtained by combining information from two separate MS4 CA-ECD experiments of the $[M+11H]^{10+\bullet}$ and $[M+11H]^{9+\bullet\bullet}$ ions respectively is presented in **Figure 20**. Collisional activation of the charge-reduced radical light chain ions generates information throughout the backbone. Both intramolecular disulfide bonds appear to be reduced, presumably during the electron capture step of the process, since information from within the SS linked domains cannot be generated in MS3 CID experiments of the light chain. It is speculated that following electron capture, both SS bonds are reduced and that non-covalent interactions preserve the folded configuration of the light chain while supplemental collisional activation is necessary to dissociate the protein into fragments. The sequence coverage obtained by analyzing two of the charge-reduced fragments is 83%. Further enhancements in sequence coverage are expected by including information from additional charge-reduced light chain ions accommodating a greater number of radical sites.

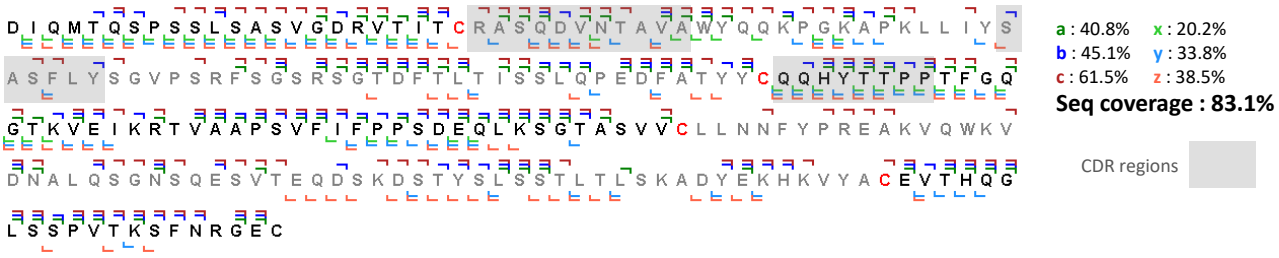

Figure 20. Sequence map of the light chain demonstrating an 83% coverage obtained in MS4 CA-ECD where selected charge-reduced light chain radical ions are dissociated via collisions with argon.

Modifications to the side chain of cysteines participating in intramolecular SS bonds were taken into consideration and a high number of primary fragments with modified side-chains on cysteine residues were identified, as shown in the sequence map of **Figure 21**. These modifications add further to the complexity of the mass spectrum originating from the dissociation pattern of the intermolecular SS bond connecting heavy and light chains, as discussed with reference to **Figure 17**. Sulfhydryl group (-SHx) additions and losses are observed for b fragments and derive from the intramolecular SS bond dissociation, enriching the fragmentation pattern (triplet configuration). Examples of the triplet fragment ion configuration on aspartic acid residues arising from the dissociation of the first intramolecular SS bond is presented in the mass spectrum of **Figure 21**. A more complicated situation arises when C-terminus fragment containing at least one cysteine participating in an intramolecular disulfide bond is identified. For these fragment ions it becomes practically impossible to distinguish if the modification on the side chain of cysteine arises due to dissociation of the intramolecular or the intermolecular SS linkage. A mass spectrum highlighting the problem is presented at the end of **Appendix II**.

The averaged signal intensity of the MS4 fragments in the Tune software (Thermo Fisher) is of the order of $\sim 10^2$, which is below the typical threshold normally used in Xcalibur (Thermo Fisher) for accurate assignments ($\sim 10^4$). These lower levels of detection in signal ion intensity were accomplished by eliminating the chemical background noise observed in the mass spectrum of the Q-Exactive mass spectrometer. To eliminate the chemical background, new instrument settings were developed to filter out ions transmitted from the ionization source and accumulated into the c-trap and ultimately in the Orbitrap mass analyzer during processing of the ions in the Omnitrap platform. The modifications applied to the Q-Exactive were necessary to enable the MS4 experiments described here where the starting averaged ion intensity of the isolated 49+ precursor ions was of the order of $\sim 10^6$ and that of the MS4 fragments of the order of $\sim 10^2$, resulting in at least four orders of magnitude range in signal ion intensity. Considering the accumulation step introduced between the MS2 and MS3 processing levels to increase the ion population by a factor of 10x, the overall dynamic range in ion intensity processed in a single MS scan is at least five orders of magnitude. The following **Figure 22** is a schematic representation of the sequential processing steps performed in the Omnitrap platform and the averaged ion intensity recorded in each step of the MS4 workflow.

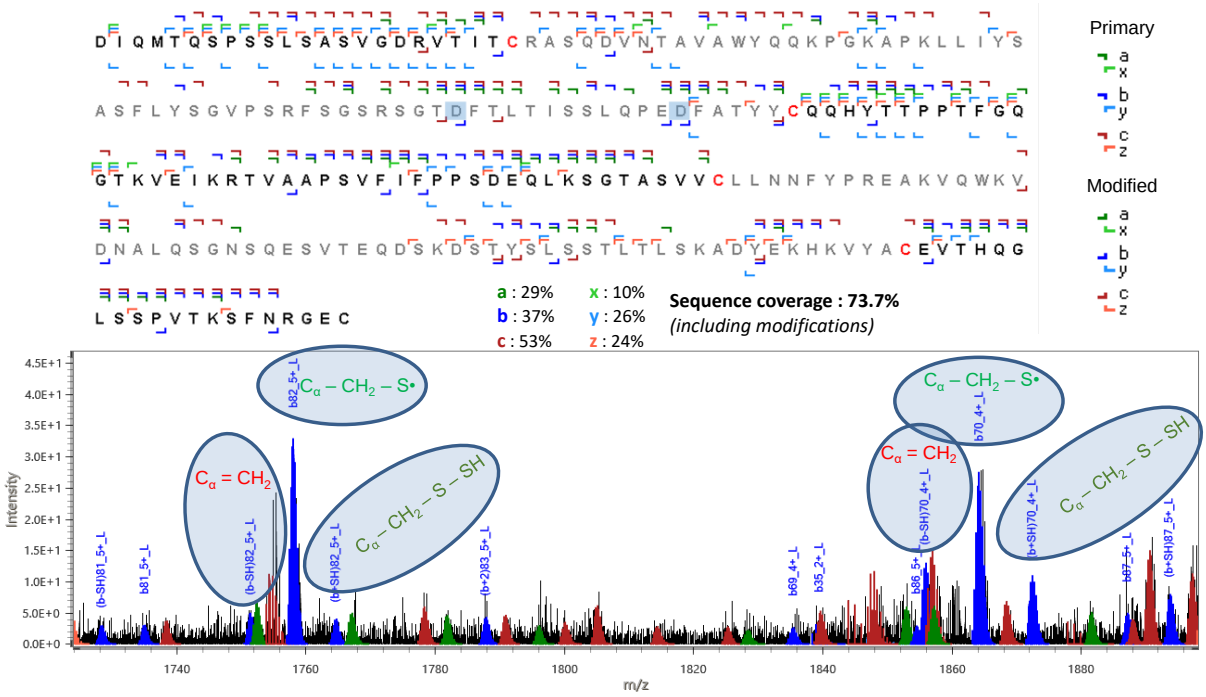

Figure 21. Sequence map of the light chain with primary fragments and cleavages accommodating the modified cysteines. Also shown is an example of a mass spectrum highlighting the triplet fragment ion configuration arising from the dissociation of the first intramolecular SS bond.

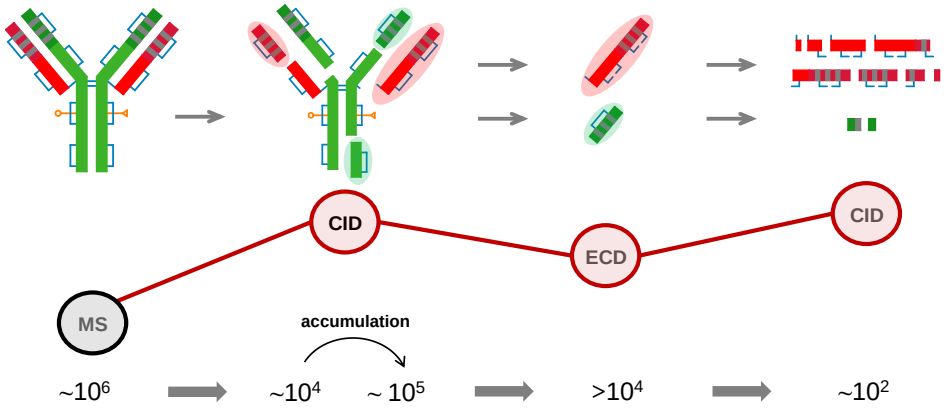

Figure 22. Schematic representation of the consecutive ion processing steps involving collisions with argon and interactions with low energy electrons. Also shown is the ion signal intensity in each step of the process.

The MS4 CA-ECD described above for the light chain was also applied for the analysis of selected N-terminus heavy chain b-type fragments. **Figure 23 (a)** shows the MS2 two-step CID mass spectrum of the 49+ intact trastuzumab ions. The b_{110}^{7+} ion of the heavy chain containing the first disulfide bridge and selected for the MS4 CA-ECD step is highlighted in the figure. Also shown is the MS3 ECD step where the charge-reduced b_{110} ions formed by electron capture are dominating the spectrum while the intensity of ECD fragments remains rather low, as observed in the top

down experiments with the light chain. The $b_{110}^{6+\bullet}$ ion selected for collisional activation at the MS4 level is also highlighted in **Figure 23 (b)**.

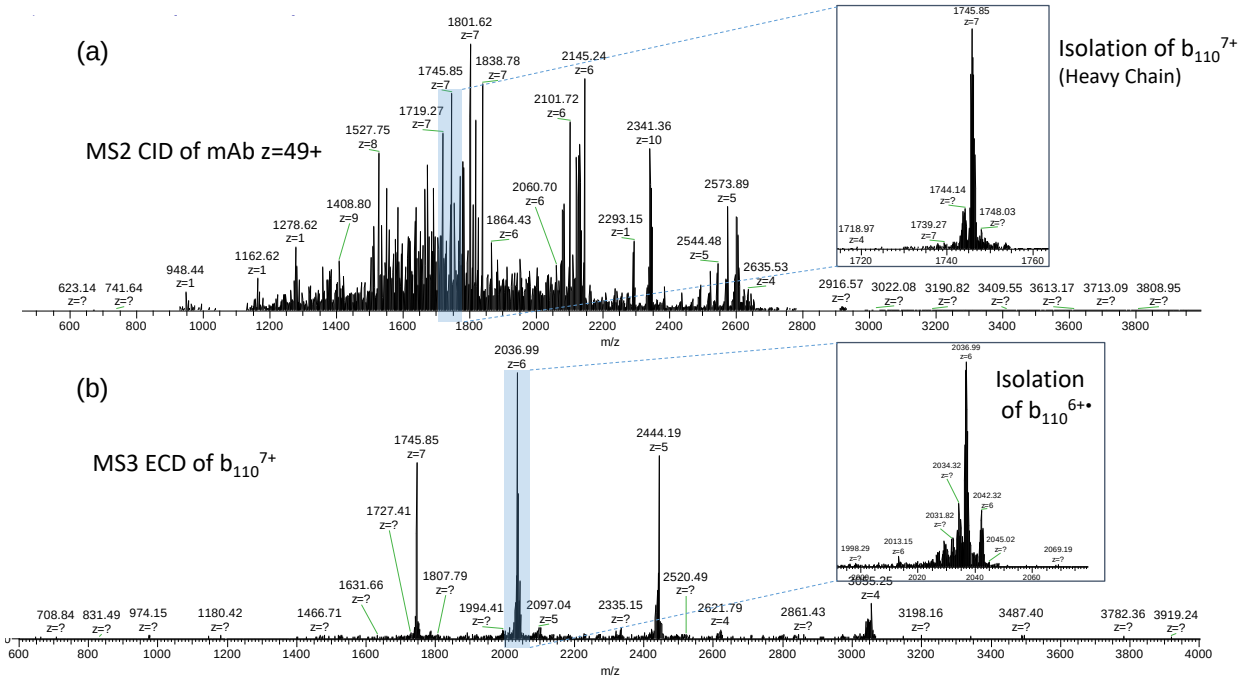

Figure 23. (a) MS2 two-step CID mass spectrum of the 49+ intact trastuzumab ions highlighting the b110 heavy chain fragment selected for further processing. (b) MS3 ECD mass spectrum of the b_{110}^{7+} ions generating charge-reduced radical ions, including the $b_{110}^{6+\bullet}$ species selected for collisional activation at MS4 level.

Figure 24 shows the MS4 slow heating CID mass spectrum generated by applying a resonance excitation signal corresponding to the secular frequency of the $b_{110}^{6+\bullet}$ ions in the presence of argon gas (>10^{-2} mbar). Manual processing of this MS4 CA-ECD mass spectrum produced a number of cleavages mainly located externally to the disulfide bridge in the variable region of the heavy chain. Additional fragments located within the SS linked domain were also identified, however, sequence coverage within the SS linked domain is considerably lower compared to the results obtained for the light chain. The overall sequence coverage for the variable region of the heavy chain is 44%, as shown in **Figure 24**. Fragment ion intensities and charge state distribution plots are also presented in **Appendix II**. Additional experiments involving collisional activation of the $b_{110}^{5+\bullet\bullet}$ ions at MS4 level have been performed and processing is underway. It must be noted that despite the manual aspect of the analysis adopted throughout this study, a significant number of the assignments in the MS4 CA-ECD experiment of the b_{110}^{7+} ions cannot be made with high confidence due to the extreme complexity of the mass spectrum.

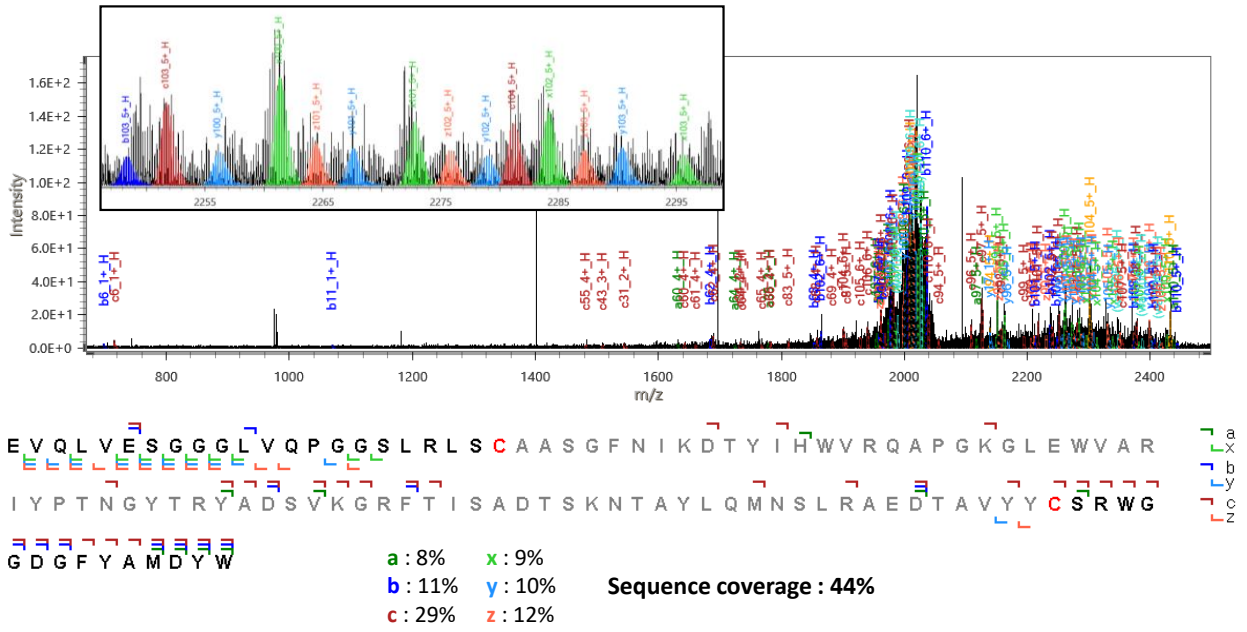

Figure 24. MS4 CA-ECD mass spectrum of the $b_{110}^{6+\bullet}$ ions of the heavy chain. The sequence map shows 44% coverage suggesting incomplete reduction of the intramolecular SS bond.

The MS4 workflow developed and described in this section is undoubtedly a powerful tool for top down analysis of intact antibodies. In this example, ion processing methods were limited to low energy electrons and slow heating collisional activation. The versatile ion activation network available in the Omnitrap platform can support the development of new multiple-stage multi-dimensional ion activation experiments involving photons, reagent ions and radical atoms at any step of the ion processing cycle. The unique nature of these analytical workflows is expected to enhance the level of information produced and the combination of the results will evidently improve sequence coverage even further. The results presented in **Figure 24** suggest that complete sequence coverage of an intact mAb in a top down experiments is clearly feasible.

1.4 MS2 Electron Induced Dissociation

The ability to control the injection energy of electrons in an ion trap with high efficiency is undoubtedly one of the unique features of the Omnitrap platform. FT-ICR is the only alternative technology that can support interactions between trapped ions and variable energy electrons. In a recent study comparing the MS2 EID performance between the two MS platforms (Omni-QE and FT-ICR), it was demonstrated that the Omnitrap is one order of magnitude faster (50 ms) while the signal-to-noise ratio of the generated spectra is also improved by another order of magnitude (ASMS 2020). The enhanced efficiency of dissociation is attributed to the stronger radial and axial confinement of the ions in the Omnitrap platform compared to the larger size the ions occupy in an ICR cell. In addition, the lower transfer efficiency of precursor ions in FT-ICR requires longer injection times to accumulate a sufficient number of ions in order to observe the low efficiency dissociation pathways normally obtained in EID.

These limitations in existing technology have precluded the study of ion activation - dissociation by high energy electrons in the higher m/z range. The combination of the Omnitrap platform (Fasmatech) with a Q-Exactive mass spectrometer upgraded with the Biopharma option (Thermo Fisher) offers a unique opportunity to explore this type of interactions with high efficiency. To the best of our knowledge, electron ionization and electron induced dissociation of intact antibodies sprayed under native conditions are reported here for the first time. **Figure 25** shows the different regimes identified by controlling the energy of electrons injected in segment Q5.

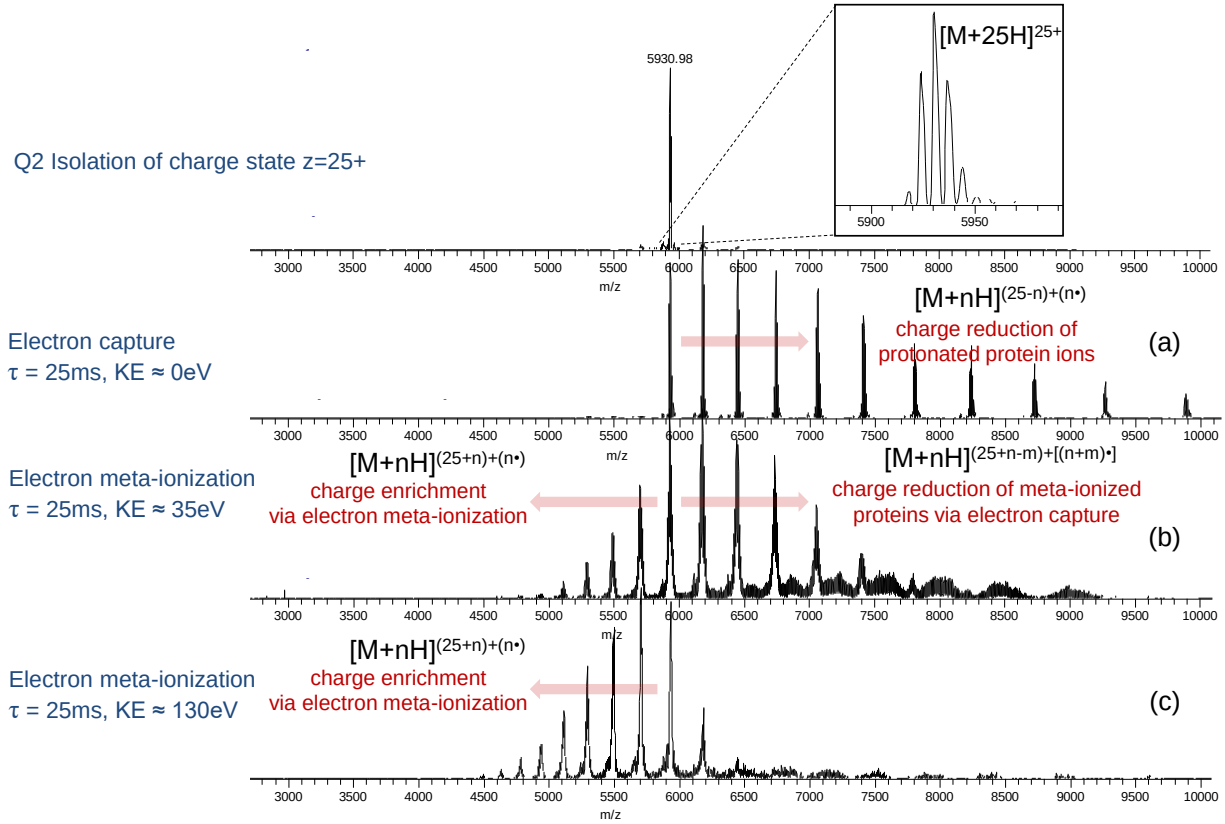

Figure 25. Different ion activation - dissociation regimes are identified as a function of electron energy. (a) Electron capture leads to the formation of charge-reduced ions, (b) ionization followed by electron capture is observed at 35 eV while (c) direct ionization is observed only for the higher electron energies.

A series of experiments were performed with different charge states of intact trastuzumab sprayed under native conditions. In the example shown in **Figure 25**, ions are isolated first in segment Q2 since the isolation window available on Q-Exactive platform is limited to ~3500 Th. Selected ions are subsequently transferred to segment Q5 and irradiated by electrons. The energy of the electrons is determined by the potential difference applied between the filament and the DC offset applied to the pole-electrodes of Q5. Different regimes can be identified by the nature of the product ions observed in the mass spectrum. Electron capture is observed by injection of low energy electrons (<10 eV) leading to the formation of charge-reduced product ions. The electron capture reaction can be written as follows:

$$[M+nH]^{n+} + m\times e^-_{<10eV} \rightarrow [M+nH]^{(n-m)+(m\bullet)} \quad (1)$$

Here, “m” represents the number of electrons captured by the multiply protonated ions whereby the precursor ion charge state “n” is reduced to (n-m) while an equal number of “m” radical sites are formed assuming no electron recombination occur due to the large size of the protein. Extending electron irradiation time will generate fragments but for the larger size proteins supplemental collisional activation is required to enhance the efficiency of dissociation as described above in Sections 1.2 and 1.3.

At 35 eV electron energy, the energy level identified experimentally to give the highest EID efficiency for small molecules, peptides and low-size proteins, two separate effects are observed. The first step appears to be direct electron meta-ionization and the reaction can be written as follows:

$$[M+nH]^{n+} + m\times e^{-}_{35eV} \rightarrow [M+nH]^{(n+m)+(m\bullet)} + m\times e^{-}_{35eV} + m\times e^{-}_{0eV} \quad (2)$$

Here “m” is the number of fast electrons knocking-off an equal number of valence electrons from the protein to increase the charge state to a value of (n+m) whereby the meta-ionized species will carry an “m” number of radical sites. A fraction “k” of the “m” number low energy electrons detached from the protein upon meta-ionization will be re-captured by the ionized species. This second step of the reaction can be written as follows:

$$[M+nH]^{(n+m)+(m\bullet)} + k\times e^{-}_{0eV} \rightarrow [M+nH]^{(n+m-k)+[(m+k)\bullet]} \quad (3)$$

This is the standard electron capture reaction (1) described above, however, in this case product ions of the same charge state will carry a greater number of radical sites (m+k) compared to the “m” number of radical sites observed in electron capture of polyprotonated even-electron species. The assumption that electron hole recombination does not occur due to the larger size of the proteins remains here too.

A comparison between an MS2 EID and an MS2 ECD experiment with native ions at the same charge state 25+ is presented in **Figure 26**. In general, all MS2 ECD experiments with native trastuzumab ions produced a relatively small number of fragments and the best sequence coverage obtained by applying a broadband excitation signal to dissociate the high-mass charge-reduced species via collisions was limited to 20% for the light chain and to 10% for the heavy chain. These results are presented in **Appendix III**. In contrast to ECD, EID produced a plethora of fragment ions over an extended mass range, as shown in **Figure 25**. Despite the rich fragmentation patterns produced in MS2 EID experiments with native trastuzumab ions, no effort was made to analyze the mass spectrum due to the extreme congestion observed throughout the mass range of interest. The majority of the isotopic distributions are largely obscured and no clear isotopic patterns are formed that would enable identifications to be made with high confidence. Additional MS2 EID experiments irradiating the entire charge state envelope of the native mAb ions with 35eV electrons, followed by broadband excitation collisional activation of the ionized- and charge-reduced intact ions to generate isotopically resolved fragments in the lower m/z region of the mass spectrum have also been performed and shown in **Figure 27**, however, no effort has been made yet to process the information. EID of native and denatured intact mAbs remains largely unexplored, despite the successful implementation of this method in the Omnitrap platform and the generation of rich information spectra at MS2 level. EID is expected to play a more important role in MS3 workflows and particularly for lower m/z ions with low charge states,

nevertheless, a more detailed study is necessary to evaluate the information contained in the spectra presented in **Figures 26** and **27**. Of great interest is also the information produced in more exotic workflows, such as the one presented in **Appendix IV** where native trastuzumab ions are irradiated by low energy electrons and the charge-reduced precursors formed by electron capture are subsequently irradiated by energetic electrons to generate EID-type fragments.

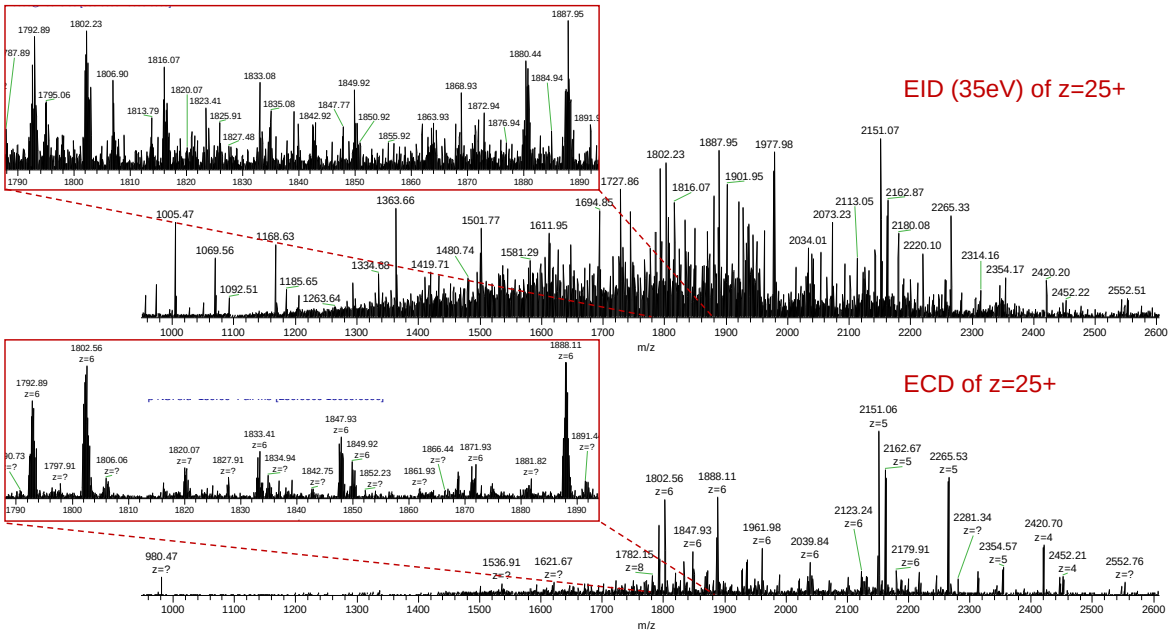

Figure 26. Spectral comparison between MS2 ECD and MS2 EID of native trastuzumab ions.

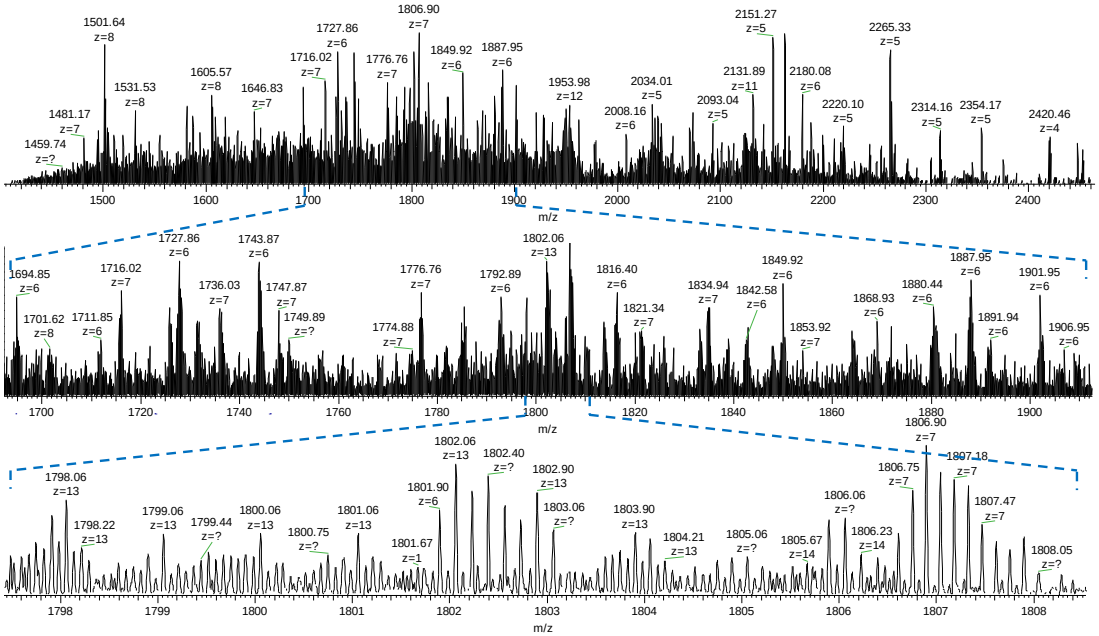

Figure 27. MS2 EID mass spectrum of all native charge states highlighting spectral congestion.

Appendix I

MS2 ECD assignments in PeakFinder

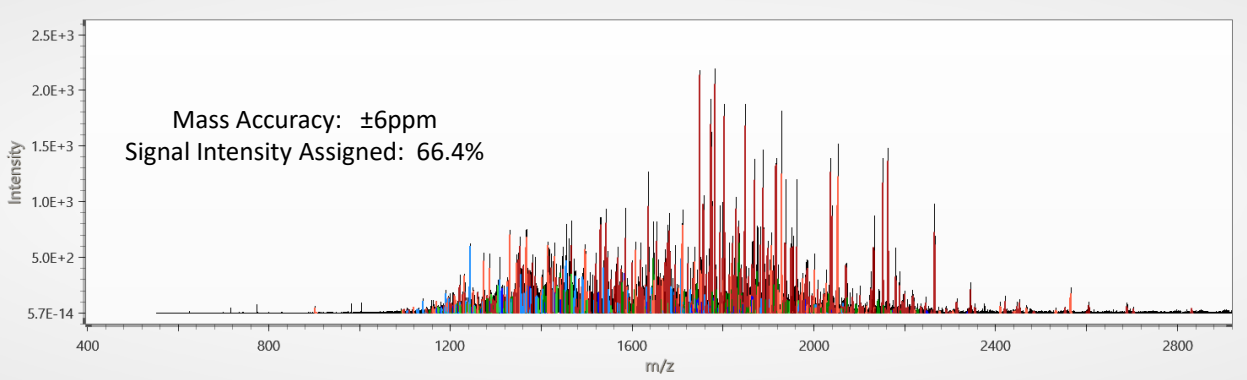

Mass Accuracy

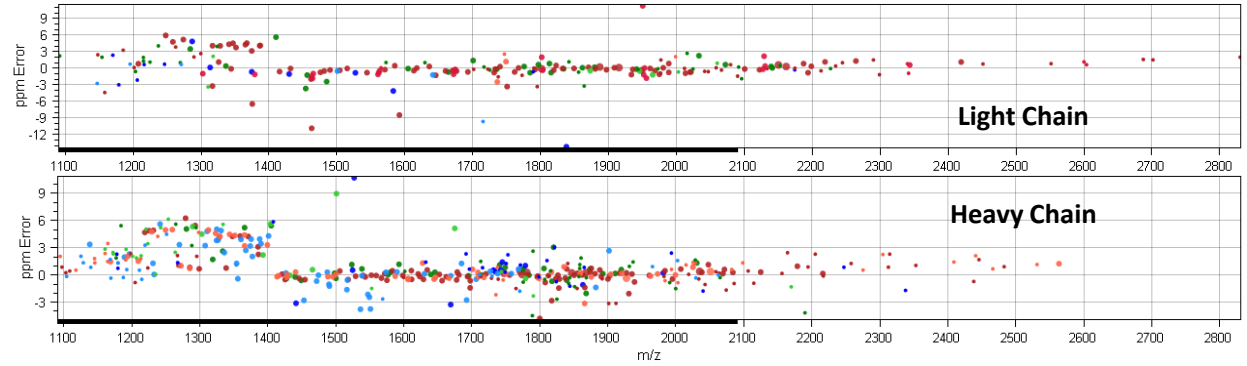

Light Chain

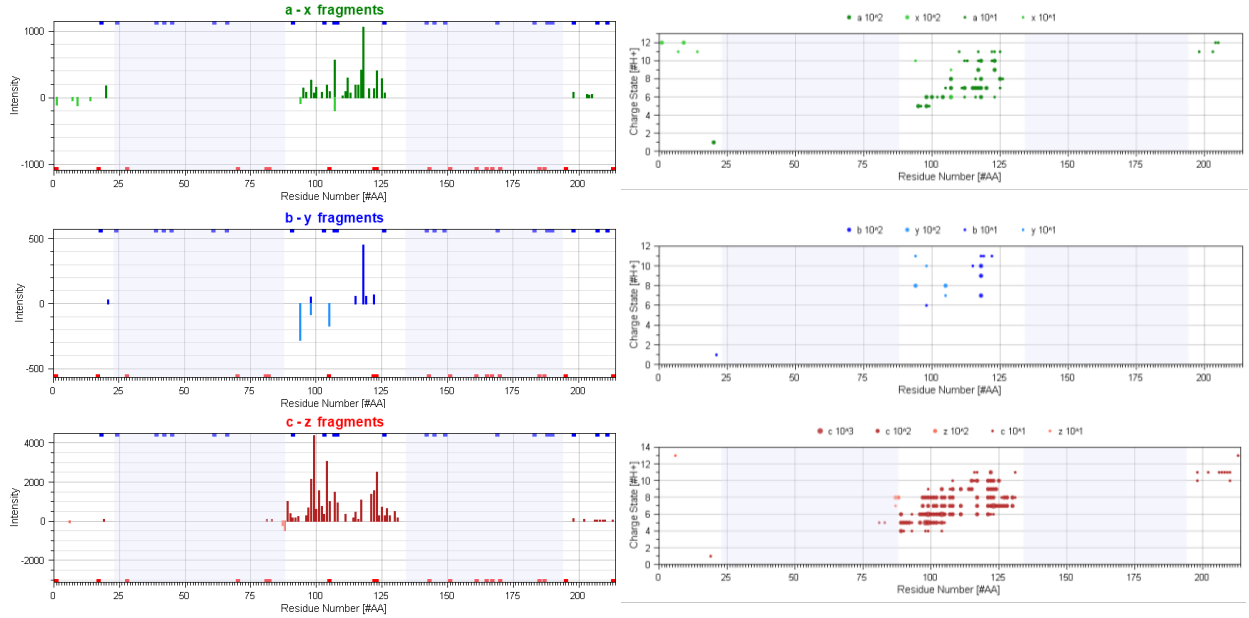

Heavy Chain

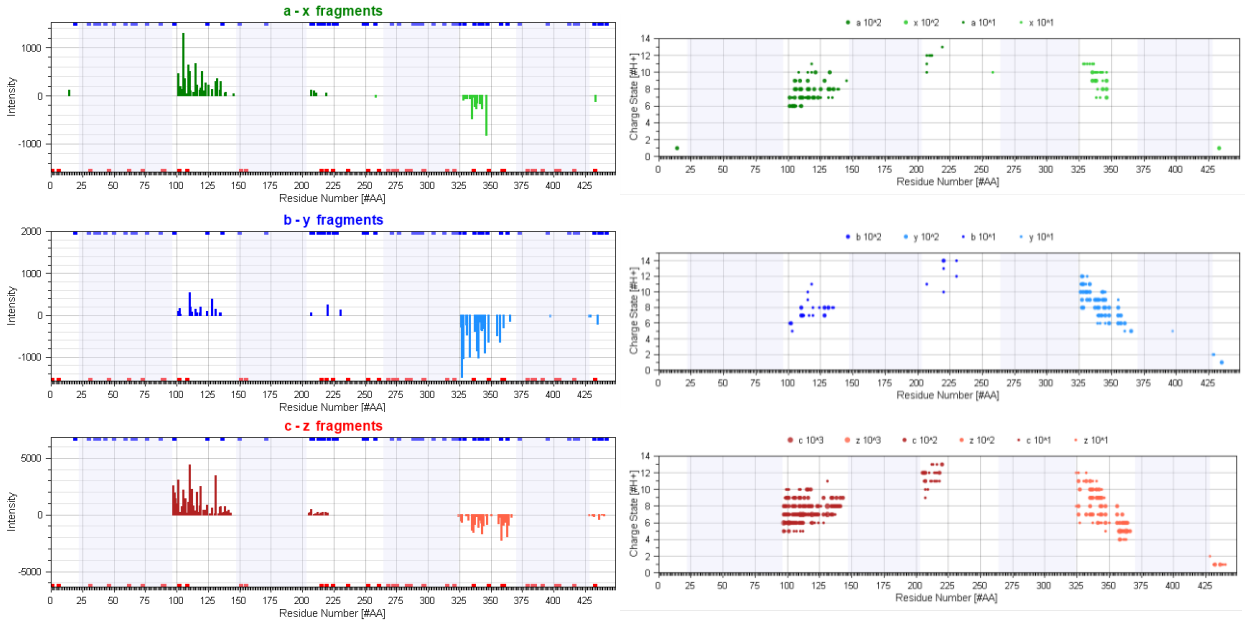

MS2 CA-ECD assignments in PeakFinder

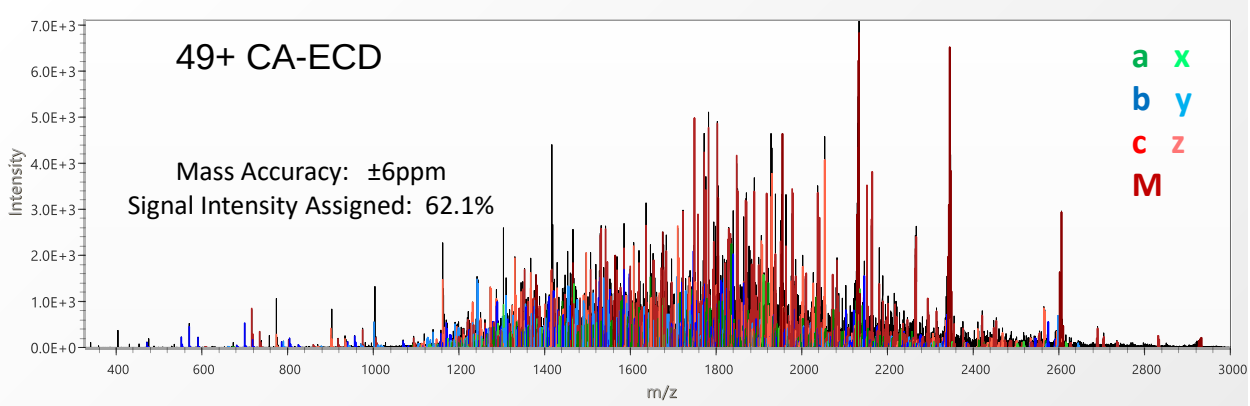

Mass Accuracy

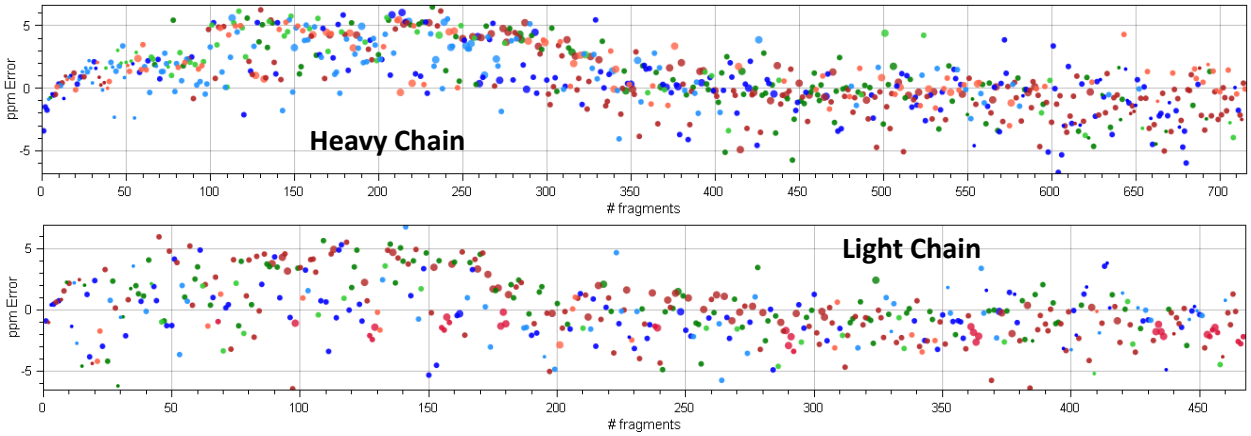

Heavy Chain

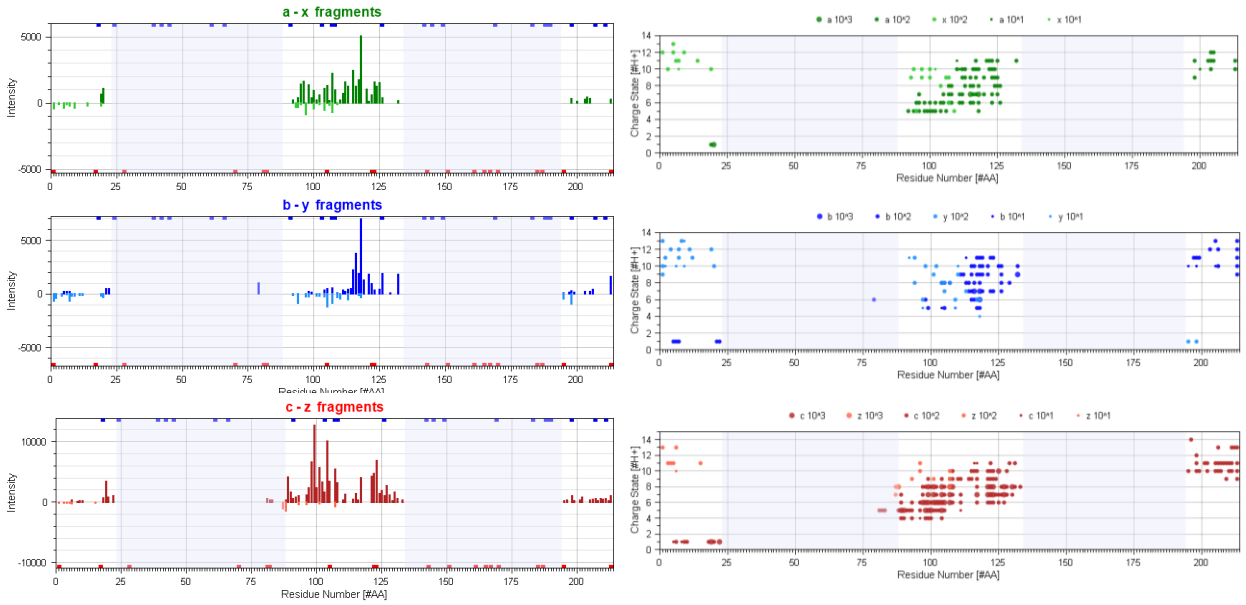

Light Chain

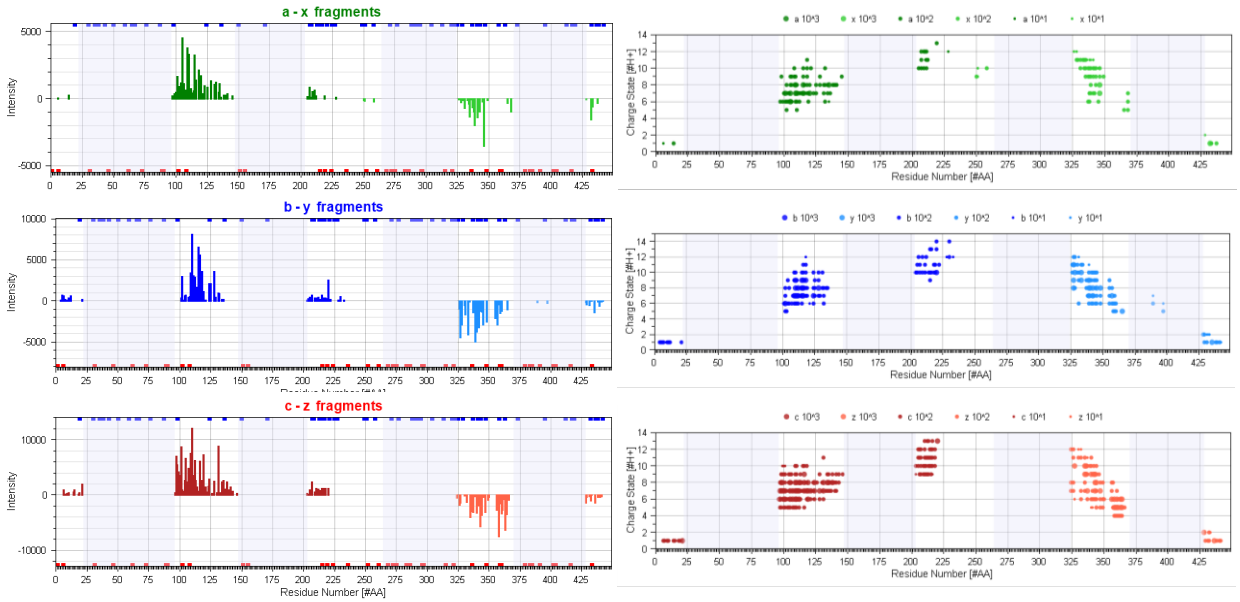
a - x fragments
b - y fragments
c - z fragments
Intensity
Charge State [#H+]
Residue Number [#AA]
a 10^3
x 10^3
a 10^2
x 10^2
a 10^1
x 10^1
b 10^3
y 10^3
b 10^2
y 10^2
b 10^1
y 10^1
c 10^3
z 10^3
c 10^2
z 10^2
c 10^1
z 10^1

Appendix II

[M+11H]$^{10+\bullet}$ *MS4 CA ECD assignments in PeakFinder*

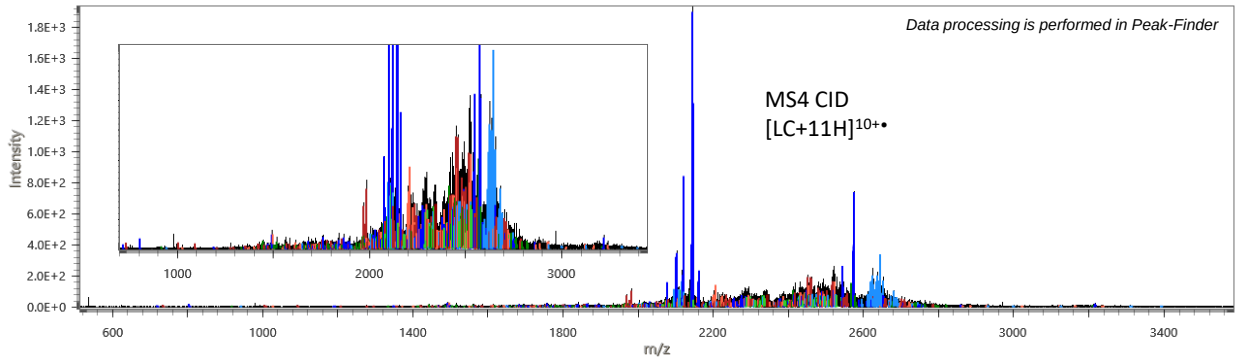

Light Chain Sequence Map

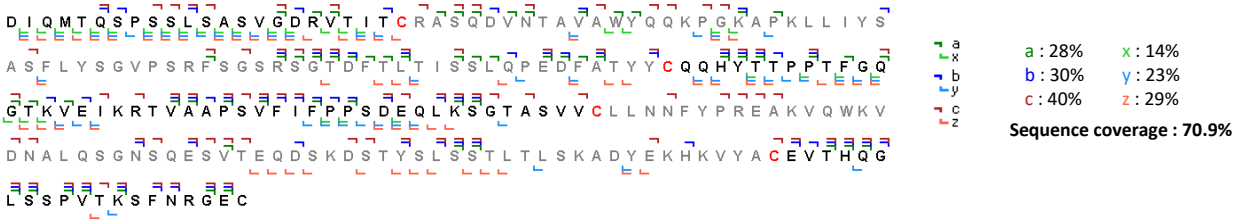

Light Chain Fragments - Intensity and Charge State Distribution Plots

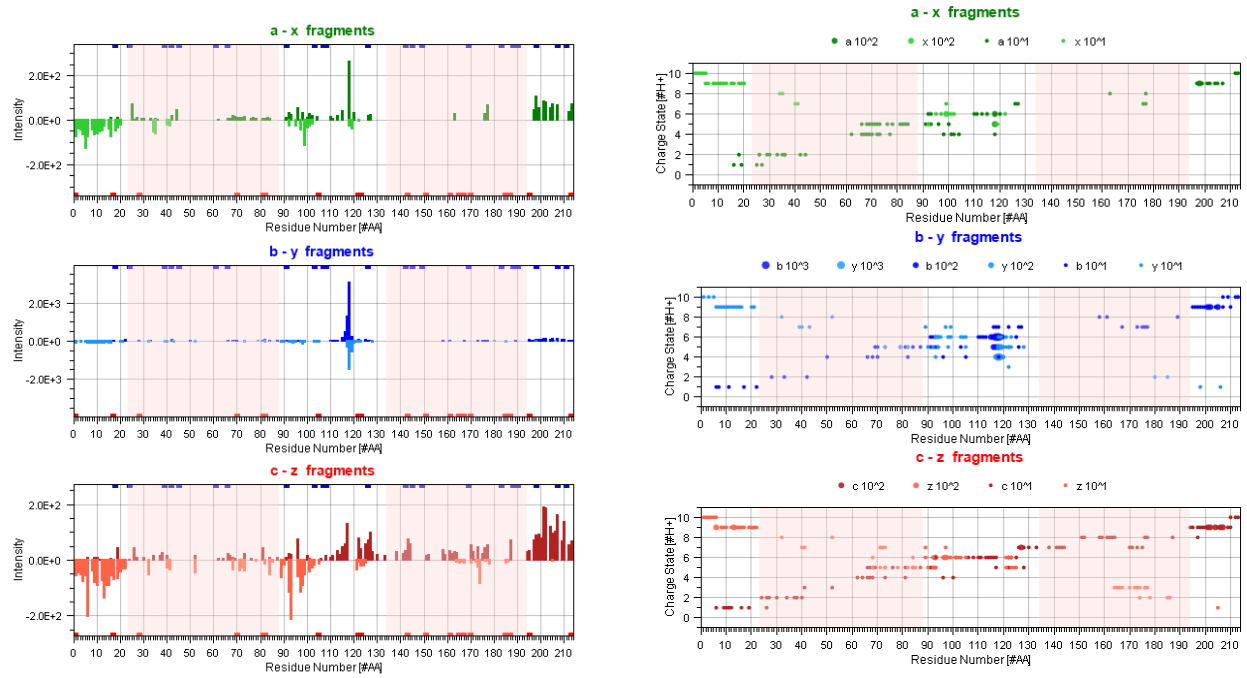

[M+11H]$^{9+\bullet\bullet}$ *MS4 CA ECD assignments in PeakFinder*

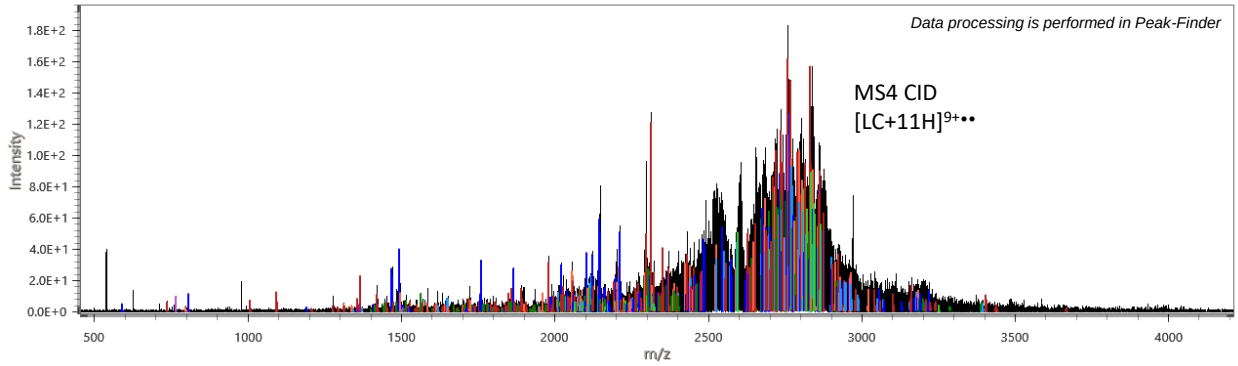

Light Chain Sequence Map

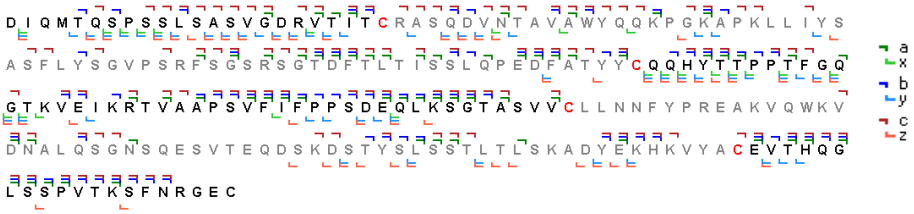

a : 29% x : 10%
b : 37% y : 26%
c : 53% z : 24%

Sequence coverage : 73.7%

Light Chain Fragments - Intensity and Charge State Distribution Plots

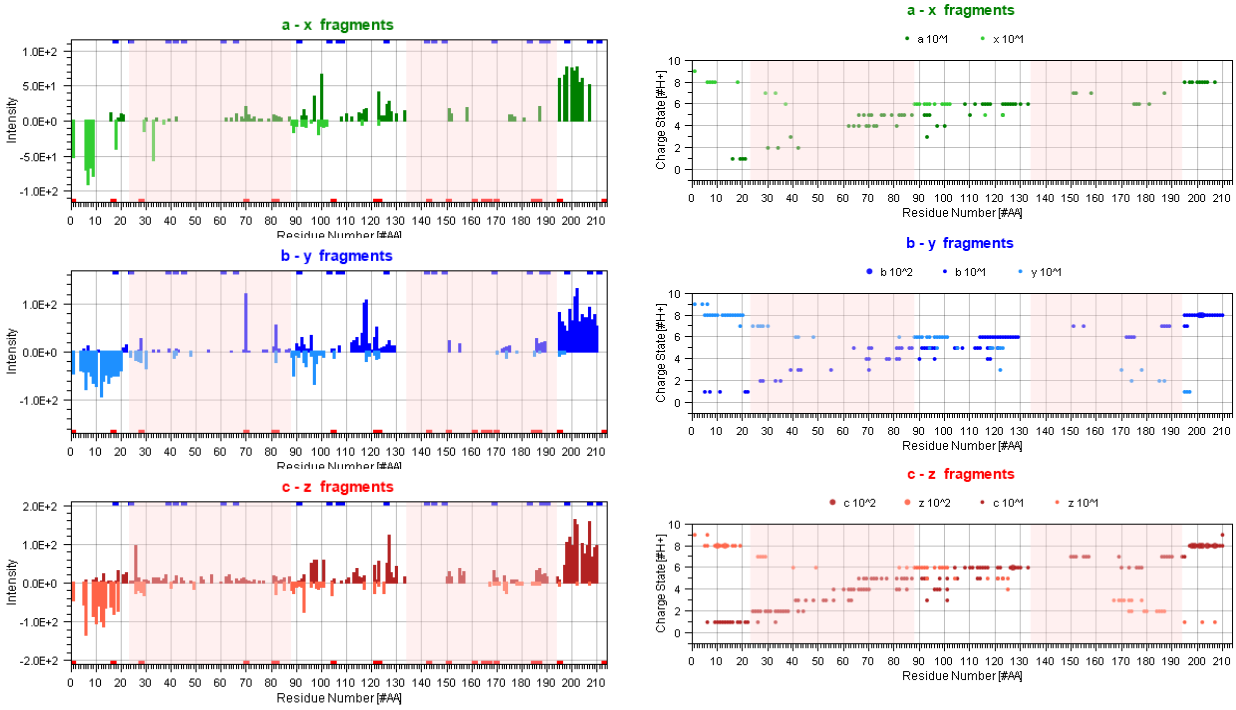

C-terminus fragments accommodating cysteine modifications

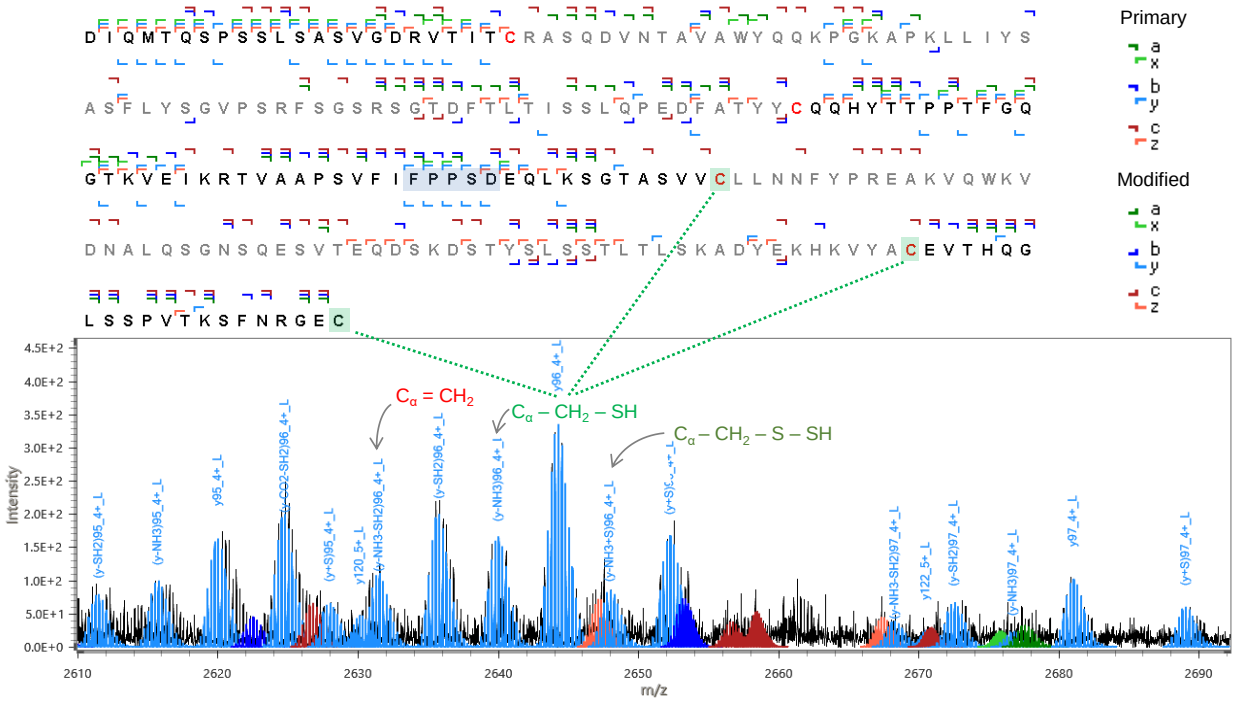

$b_{110}^{6+\bullet}$ *MS4 CA ECD assignments in PeakFinder*

$b_{110}^{6+\bullet}$ Heavy Chain Fragments - Intensity and Charge State Distribution Plots

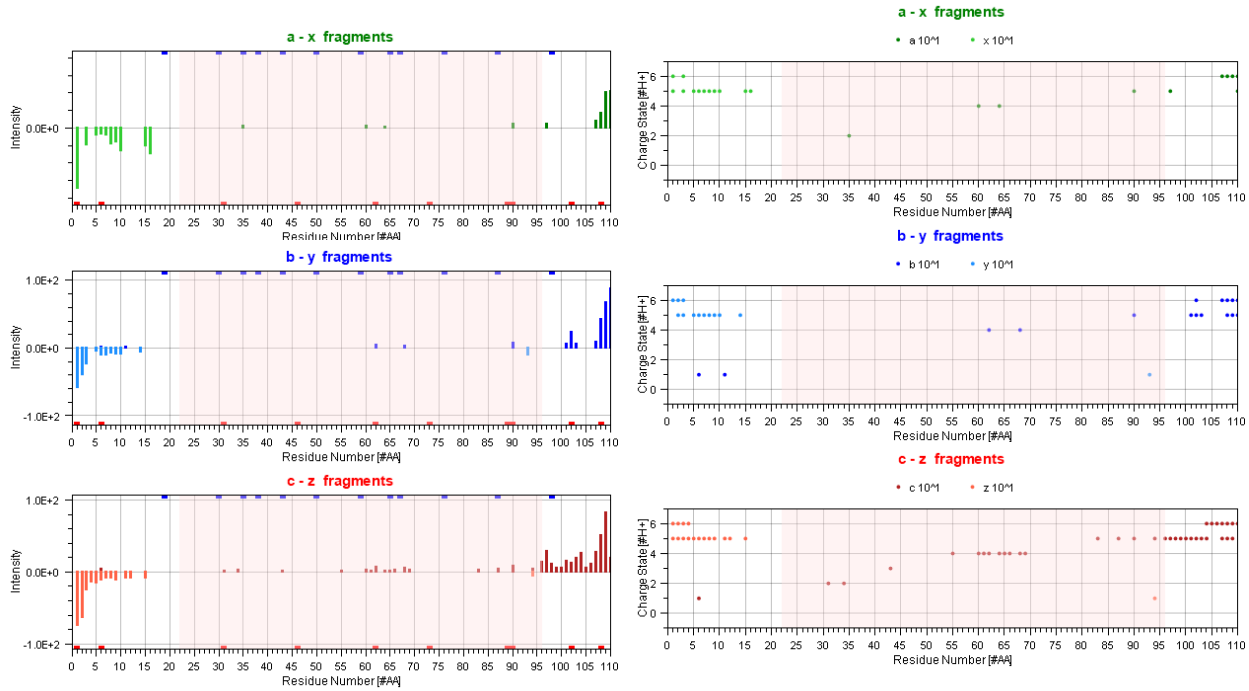

Appendix III

MS2 ECD of Native $[M+25H]^{25+}$

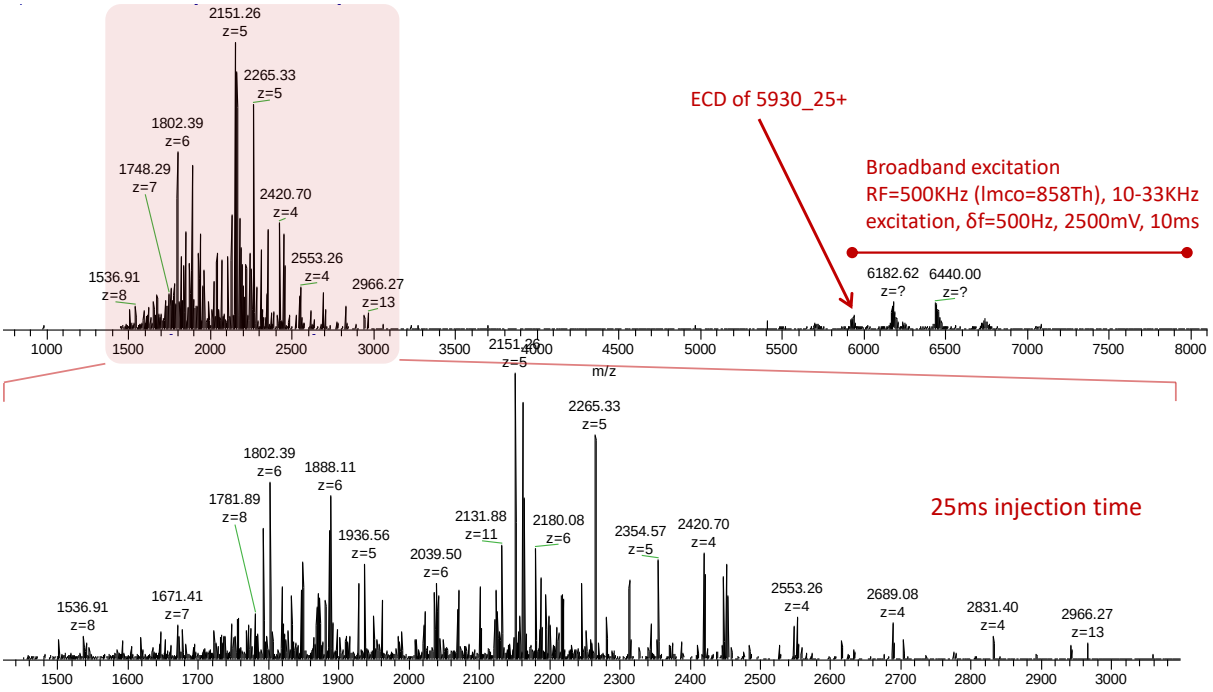

MS2 ECD assignments in PeakFinder

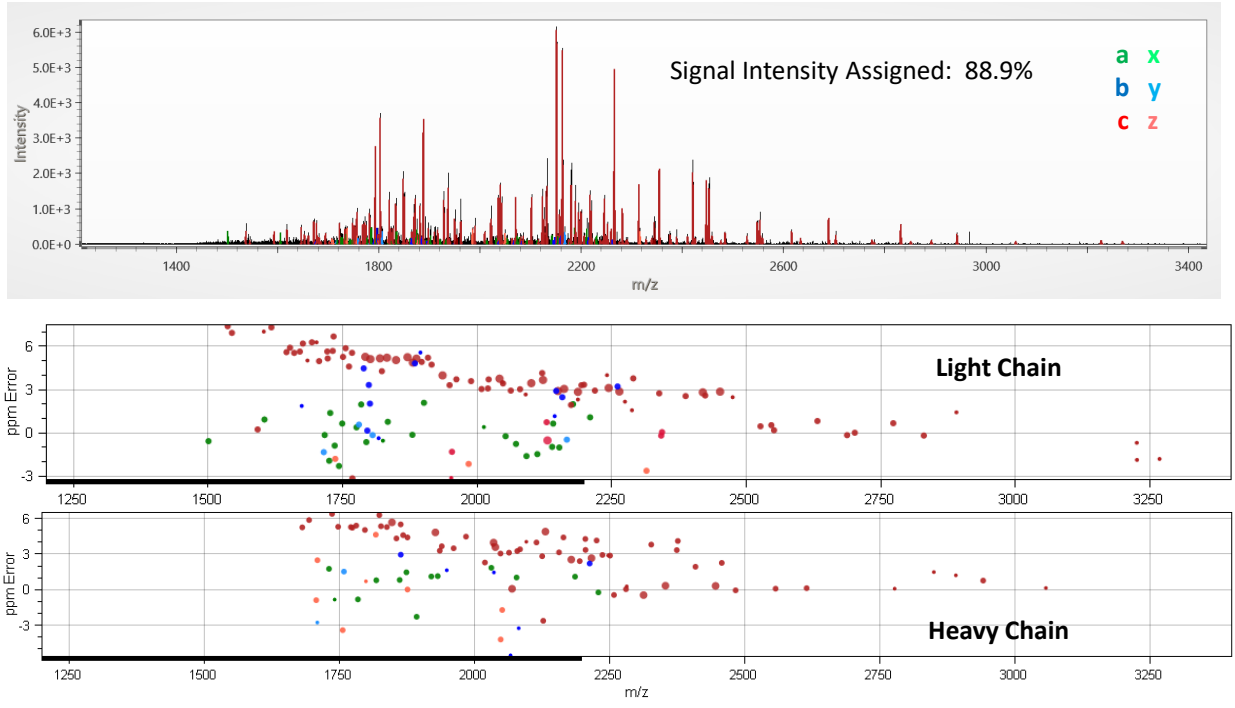

Sequence Map

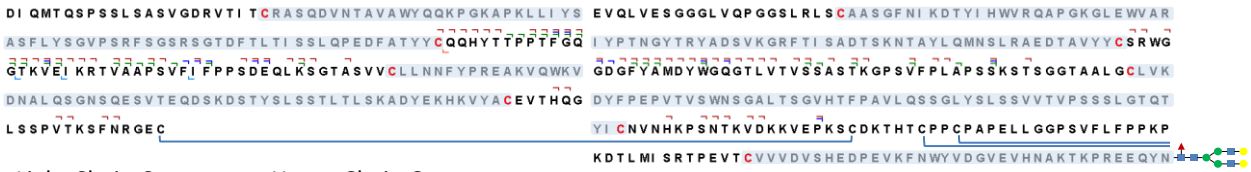

Light Chain Coverage		Heavy Chain Coverage	
a : 8.4%	x : 0%	a : 2.2%	x : 0%
b : 3.7%	y : 1.4%	b : 1.3%	y : 0.4%
c : 17.3%	z : 0.5%	c : 7.8%	z : 1.6%
Total: **20.1%**		Total: **10.0%**	

Intensity and Charge State Distribution Plots – Light Chain

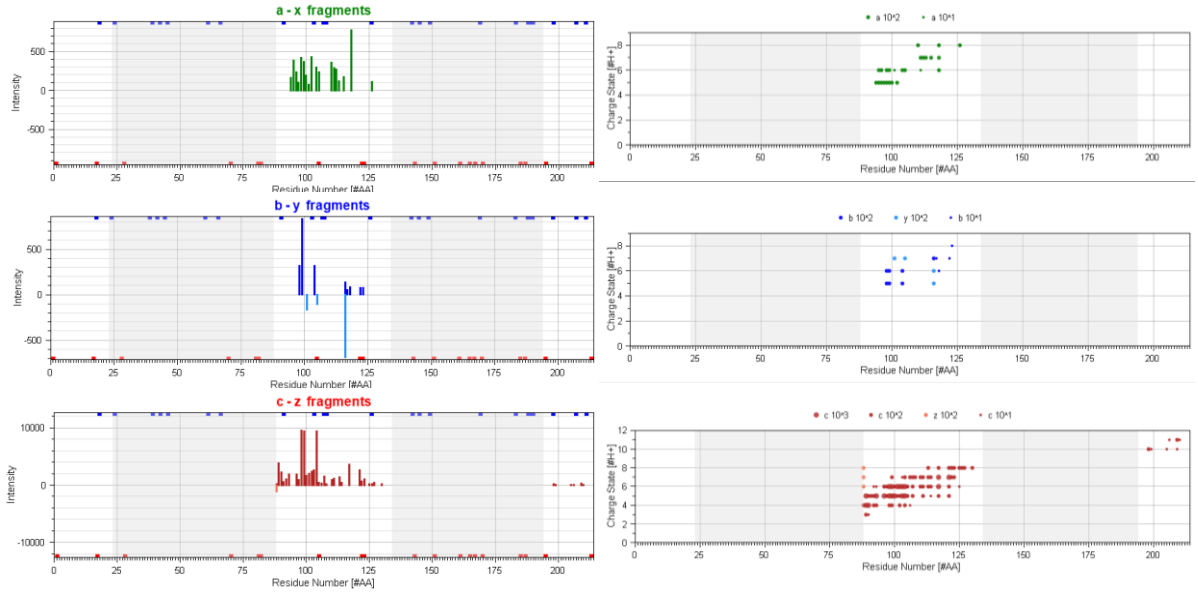

Intensity and Charge State Distribution Plots – Light Chain

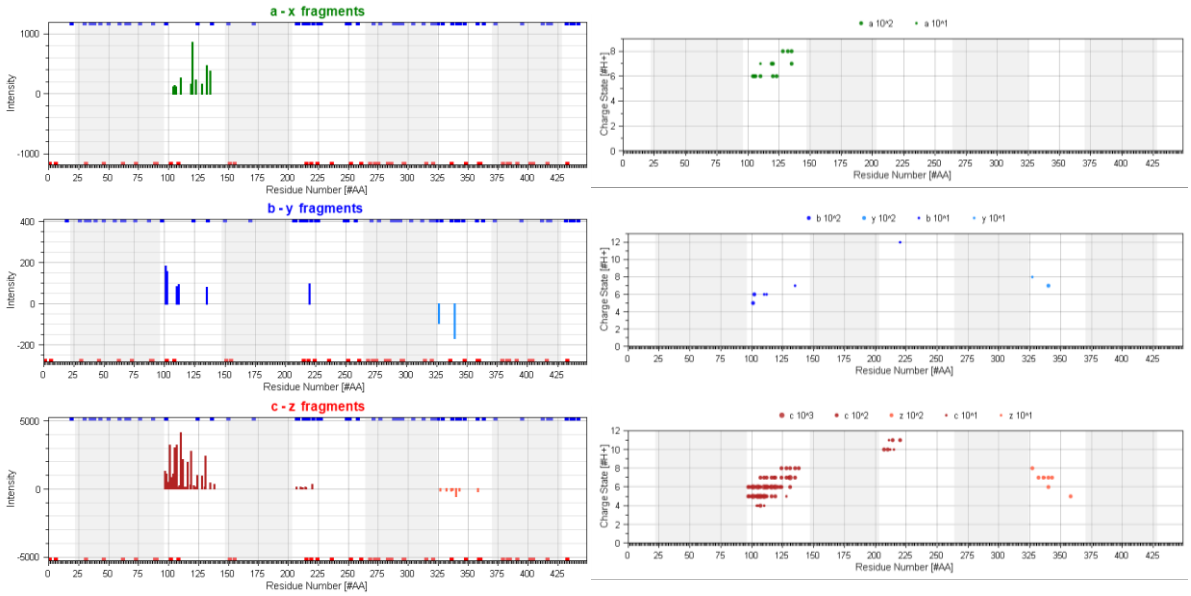

Appendix IV

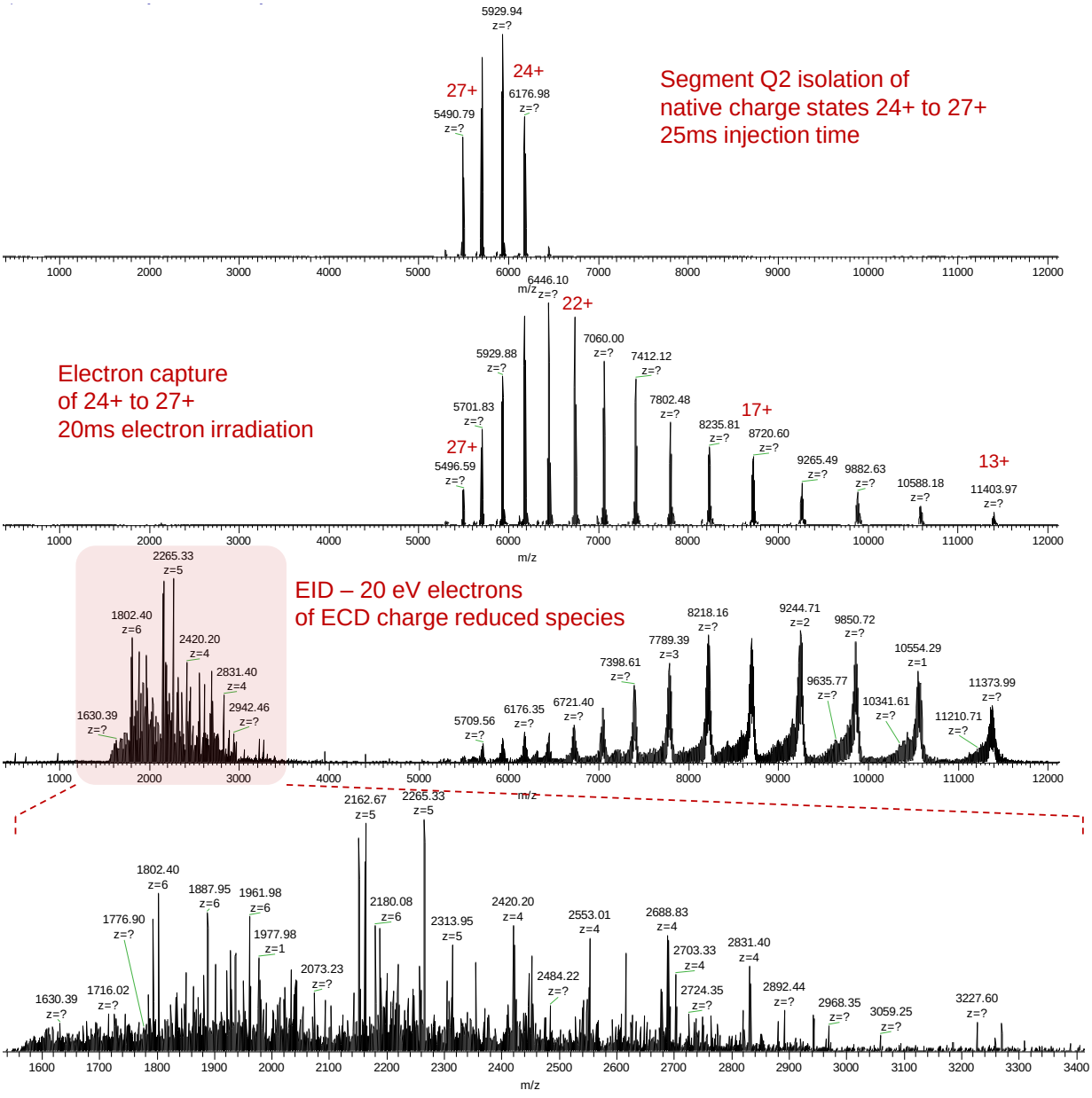
Segment Q2 isolation of
native charge states 24+ to 27+
25ms injection time
Electron capture
of 24+ to 27+
20ms electron irradiation
EID – 20 eV electrons
of ECD charge reduced species
m/z